



HAL
open science

Protist community composition during early phytoplankton blooms in the naturally iron-fertilized Kerguelen area (Southern Ocean)

C. Georges, S. Monchy, S. Genitsaris, U. Christaki

► **To cite this version:**

C. Georges, S. Monchy, S. Genitsaris, U. Christaki. Protist community composition during early phytoplankton blooms in the naturally iron-fertilized Kerguelen area (Southern Ocean). *Biogeosciences*, 2014, 11 (20), pp.5847-5863. 10.5194/bg-11-5847-2014 . insu-03324647

HAL Id: insu-03324647

<https://insu.hal.science/insu-03324647v1>

Submitted on 23 Aug 2021

HAL is a multi-disciplinary open access archive for the deposit and dissemination of scientific research documents, whether they are published or not. The documents may come from teaching and research institutions in France or abroad, or from public or private research centers.

L'archive ouverte pluridisciplinaire **HAL**, est destinée au dépôt et à la diffusion de documents scientifiques de niveau recherche, publiés ou non, émanant des établissements d'enseignement et de recherche français ou étrangers, des laboratoires publics ou privés.



Distributed under a Creative Commons Attribution 4.0 International License



Protist community composition during early phytoplankton blooms in the naturally iron-fertilized Kerguelen area (Southern Ocean)

C. Georges, S. Monchy, S. Genitsaris, and U. Christaki

INSU-CNRS, UMR8187 LOG, Laboratoire d'Océanologie et de Géosciences, Université du Littoral Côte d'Opale, ULCO, 32 avenue Foch, 62930 Wimereux, France

Correspondence to: U. Christaki (urania.christaki@univ-littoral.fr)

Received: 18 June 2014 – Published in Biogeosciences Discuss.: 21 July 2014

Revised: 16 September 2014 – Accepted: 17 September 2014 – Published: 21 October 2014

Abstract. Microbial eukaryotic community composition was examined by 18S rRNA gene tag pyrosequencing, during the early phase of spring phytoplankton blooms induced by natural iron fertilization, off Kerguelen Island in the Southern Ocean (KEOPS2 cruise). A total of 999 operational taxonomical units (OTUs), affiliated to 30 known high-level taxonomic groups, were retrieved from 16 samples collected in the upper 300 m water column. The alveolata group was the most abundant in terms of sequence number and diversity (696 OTUs). The majority of alveolata sequences were affiliated to Dinophyceae and to two major groups of marine alveolates (MALV-I and MALV-II). In the upper 180 m, only 13 % of the OTUs were shared between of the fertilized stations and the reference site characterized by high-nutrient low-chlorophyll (HNLC) waters. Fungi and Cercozoa were present in iron-fertilized waters, but almost absent in the HNLC samples, while Haptophyta and Chlorophyta characterized the HNLC sample. Finally, the 300 m depth samples of all stations were differentiated by the presence of MALV-II and Radiolaria. Multivariate analysis, examining the level of similarity between different samples, showed that protistan assemblages differed significantly between the HNLC and iron-fertilized stations, but also between the diverse iron-fertilized blooms.

saprophytes, parasites and intracellular symbionts (e.g. Guilou et al., 2008; Massana and Pedrós-Alió, 2008; Bråte et al., 2012). The wide ecological roles of protists include: phototrophic and mixotrophic species, belonging to the primary producers; heterotrophic species, acting as a “link” between the microbial food web and the higher trophic levels, as well as decomposers and parasitic taxa (Caron et al., 2009 and references therein). A series of molecular studies have examined spatial or temporal patterns in protistan community structure and diversity. These have indicated that the microbial community structure is generally highly responsive to environmental forcing, and that dominant protistan taxa can differ markedly over temporal and spatial scales associated with common oceanographic features (e.g. Countway et al., 2007, 2010; Nolte et al., 2010; Gilbert et al., 2012; Mangot et al., 2013; Lie et al., 2013; Wolf et al., 2014; Christaki et al., 2014).

The Southern Ocean has a unique geography with several large-scale water masses separated by oceanic fronts, and has major implications for the global ocean circulation and climate system. It is also the largest high-nutrient low-chlorophyll (HNLC) ocean, in which iron limits phytoplankton production, resulting in a large stock of major inorganic nutrients (Martin and Fitzwater, 1990). A pronounced shift to larger phytoplankton cells, in particular diatoms, has been generally observed resulting in natural (Blain et al., 2007; Pollard et al., 2009) or artificial (Boyd et al., 2007; Smetacek et al., 2012) iron additions. While evidence of iron limitation of phytoplankton growth is unequivocal, the subsequent direct or indirect impact of iron on heterotrophic eukaryotes of the microbial food web is less clear. For example, a moderate increase in microzooplankton biomass was

1 Introduction

Molecular investigations into the planktonic protists of natural microbial communities have revealed an astonishing diversity (e.g. Caron et al., 2012 and references therein) and a variety of novel and/or previously unobserved groups of

Table 1. Brief description of the stations. The depth of the mixed layer (ML) is based on a difference in sigma of 0.02 to the surface value. The mean ML (\pm SD) of all CTD casts performed during the occupation of the stations is given. Ze: the euphotic layer depth. For Chl *a* and major inorganic nutrients mean values \pm SD for the mixed layer.

Station	Date (2011)	Latitude ($^{\circ}$ N)	Longitude ($^{\circ}$ E)	Station depth (m)	Sampling depths (m)	ML (m)	Ze (m)	Chl <i>a</i> ($\mu\text{g L}^{-1}$) ^a	NO ₃ + NO ₂ (μM) ^b	PO ₄ (μM) ^b	Si(OH) ₄ (μM) ^c	DFe (nM) ^d
R-2	26 Oct	-50.359	66.717	2450	20, 60, 150, 300	105 \pm 15	92	0.25 \pm 0.08	26.0 \pm 0.2	1.83 \pm 0.03	12.3 \pm 0.3	0.08 \pm 0.07
F-L	7 Nov	-48.505	74.614	2690	20, 65, 180, 300	38 \pm 7	28	4.00 \pm 1.58	20.5 \pm 1.9	1.06 \pm 0.21	7.7 \pm 0.8	0.22 \pm 0.06
E-4W	10 Nov	-48.765	71.425	1398	30, 80, 150, 300	61 \pm 11	31	2.38 \pm 0.31	25.4 \pm 1.0	1.79 \pm 0.10	18.5 \pm 1.2	0.17 \pm 0.03
A3-2	16 Nov	-50.624	72.056	528	20, 80, 160, 300	153 \pm 15	38	2.03 \pm 0.33	26.2 \pm 0.4	1.78 \pm 0.03	18.9 \pm 0.5	0.16 \pm 0.03

^a Lasbleiz et al. (this volume), ^b Blain et al. (this volume), ^c Closset et al. (this volume), ^d Quéroué et al. (unpublished KEOPS2 data).

observed during the iron fertilization experiment IronEx-2 in the Equatorial Pacific sector and the SOIREE in the Southern Ocean (Landry et al., 2000; Hall and Safi, 2001). In contrast, the microzooplankton grazing pressure on the total phytoplankton community decreased during the iron fertilization experiment SERIES in the Gulf of Alaska and the SEEDS1 in the western subarctic Pacific (Boyd et al., 2004; Saito et al., 2005). In the Kerguelen region, the iron limitation of the Southern Ocean is relieved by natural iron fertilization (Blain et al., 2007). Natural iron fertilization is an uncommon process in which iron supply of the surface waters from iron-rich deep water is observed. Only two studies referred to natural iron fertilization in the vicinity of Crozet (POLLARD et al., 2009) and Kerguelen Islands (Blain et al., 2007). The KEOPS 1 cruise demonstrated that the phytoplankton bloom was sustained by iron supply from iron-rich deep water below, representing natural iron fertilization (Blain et al., 2007). This study also showed that microzooplankton grazing was an important factor for phytoplankton biomass decrease in the bloom area (Brussaard et al., 2008) mainly affecting the small-sized phytoplankton population (Brussaard et al., 2008; Christaki et al., 2008).

The KEOPS2 cruise sampling strategy covered spatially diverse iron-fertilized stations at early bloom stages in the Kerguelen plateau and ocean region (October–November 2011). These data showed that natural iron fertilization of the Southern Ocean on the scale of hundreds of thousands of square kilometres produced a mosaic of blooms, and that the biological and biogeochemical response to fertilization was diverse.

The objective of this study was to explore the microbial eukaryotic community structure using 18S rRNA gene tag pyrosequencing during the onset of spring phytoplankton blooms in the context of natural iron fertilization of the Southern Ocean. The hypothesis tested was that the protistan communities would differ between the blooms, and between the iron-fertilized blooms and the HNLC waters. The use of tag pyrosequencing provided a unifying approach for assessing the breadth of protistan communities, including the groups that are quasi-impossible to characterize using traditional approaches of microscopy and culture (e.g. MAST, MALV, Fungi, and others).

2 Materials and methods

2.1 Sample collection and DNA extraction

The present study was carried out during the KEOPS2 cruise from October 15 to 20 November 2011. Water samples were collected from four stations above and off the Kerguelen plateau (Fig. 1a, b). Stations A3-2, E-4W, and F-L were located in the blooms, while the reference station R-2 was located in the HNLC region (Fig. 1a, b). All water samples were collected with 12 L Niskin bottles mounted on a rosette equipped with a CTDO Seabird SBE911-plus. According to CTD profiles, four sampling depths were chosen at each station in order to represent the mixed layer (ML), the bottom of the ML, and the deeper waters (Table 1). Five to 7.5 litres of each depth were subsequently filtered on 10, 3, and 0.6 μm , 47 mm nucleopore filters (Whatman, USA) using a serial filtration system at very low pressure (15 rpm). The serial filtration was performed in order to avoid filter clumping and to minimize disruption of fragile protists. The filters were immediately frozen in liquid nitrogen and then stored at -80°C until analysis. After pooling together and cutting into small pieces the 10, 3, and 0.6 μm filters, DNA extractions were carried out using the MO BIO PowerWater DNA Isolation Kit (MO BIO Laboratories, Inc, Carlsbad, CA), following the manufacturer's protocol instructions.

2.2 PCR and tag pyrosequencing

The DNA samples were amplified using the two universal eukaryote primers 18S-82F (5'-GAACTGCGAATGGCTC-3', López-García et al., 2003) and Euk-516r (5'-ACCAGACTTGCCCTCC-3', Amann et al., 1990). These primers have been designed to amplify the variable V2 and V3 eukaryote 18S rRNA gene regions. A 10 bp tag sequence specific to each sample, a 4 bp TCAG key, and a 26 bp adapter for the GS FLX technology, were added to the primers. Polymerase chain reactions were carried out according to standard conditions for Platinum Tag High-Fidelity DNA polymerase (Invitrogen) with 10 ng of environmental DNA as a template. After the denaturation step at 94°C for 2 min, 30 cycles of amplification were performed with a GeneAmp PCR System Apparatus (Applied

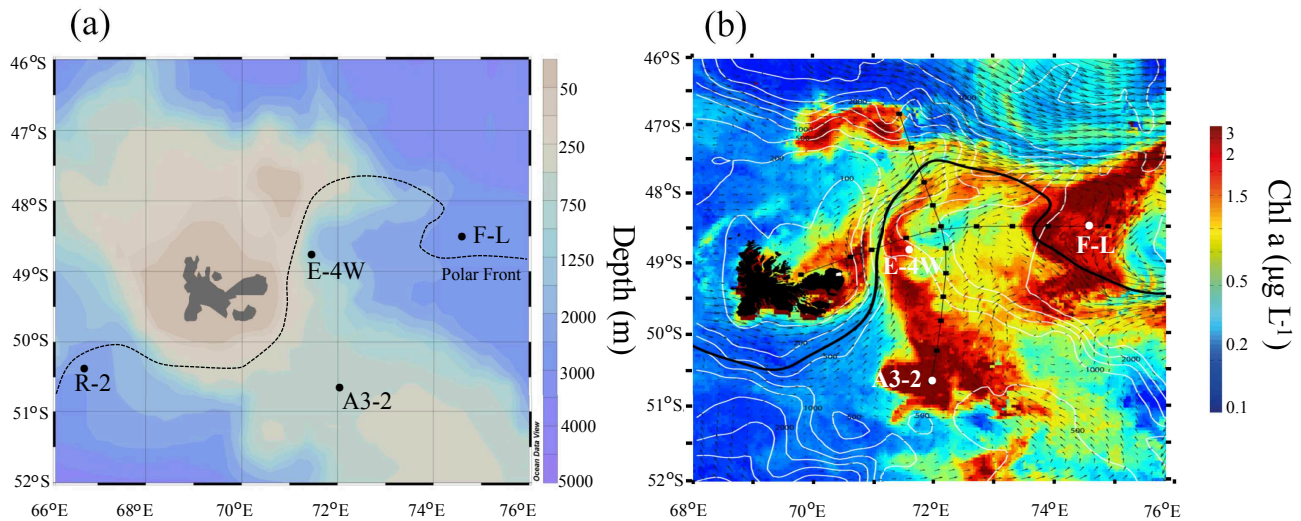


Figure 1. Bathymetry of the study area and location of the sampled stations (a), and Chl *a* (colour scale), surface velocity fields (arrows), the polar front (PF, black line) (b). The chlorophyll content represented on the map corresponds to the last week of the KEOPS2 and the cross indicates the position of the north–south and east–west transects sampled to provide an overview of the blooms. Map is courtesy of Y. Park and colleagues.

Biosystems) as follows: 15 s at 94 °C, 30 s at 50 °C, 1 min at 72 °C, and 7 min at 72 °C. Tag pyrosequencing was carried out by the company GenoScreen (Lille, France). The library was prepared following the procedures described by Roche (Basel, Switzerland) and used in a 1/4 plate run on a 454 GS FLX Titanium sequencer. Pyrosequences were submitted on GenBank-SRA under the accession number SRP041236.

2.3 Quality filtering and taxonomic affiliations of the sequences

The sequences were processed using the MOTHUR 1.28.0 software (Schloss, 2009) following the standard operating procedure (http://www.mothur.org/wiki/Schloss_SOP) (Schloss et al., 2011). First, flowgrams were extracted and demultiplexed according to their tag. The resulting 16 flowgrams were denoised using the MOTHUR 1.28.0 implementation of PyroNoise (Quince, 2009). Primer sequences, TAG and key fragments were subsequently removed, and only sequences above 200 bp long, displaying less than eight homopolymers, were kept. The remaining sequences were dereplicated to unique sequences and aligned against the SILVA 108 database (<http://www.arb-silva.de/>) containing 62 587 eukaryotes SSU-18S rRNA sequences. Around 7 % of the sequences suspected of being chimeras were removed using the UCHIME software (http://drive5.com/usearch/manual/uchime_algo.html) (Edgar, 2011). The remaining sequences were clustered into operational taxonomical units (OTUs) at 97 % similarity threshold. Single singletons (unique amplicons after 97 % clustering that occurred exclusively in only one sample) were removed from downstream analyses, as these are most likely erroneous sequenc-

ing products (Reeder and Knight, 2009; Kunin et al., 2010; Behnke et al., 2010). This data set showed a representative overview of the diversity as indicated by the rarefaction curves reaching a plateau in most cases (Supplement Fig. S1). All OTUs were given a putative taxonomic affiliations based on BLAST (Altschul et al., 1990) identification of the closest cultured or uncultured relatives against the PR2 (Guillou et al., 2013) and the GenBank databases. The OTUs identified as metazoan were removed from downstream analysis. However, the metazoan OTUs displayed high and heterogeneous number of sequences between samples, making subsampling of the remaining OTUs unsuitable as it resulted in a drastic loss of diversity. For this reason, the data are presented based on the relative abundance of OTUs in each sample.

2.4 Data analysis

Rarefaction curves and alpha diversity estimators within particular samples (richness estimator S_{Chao1} ; the heterogeneity of the diversity; Simpson and Berger–Parker indices) were calculated with the PAST 2.17c software (Hammer et al., 2001). The S_{Chao1} approach uses the numbers of singletons and doubletons to estimate the number of expected species. According to S_{Chao1} , “missing” species information is mostly concentrated on those of low frequency counts. The Simpson index measures the “evenness” of the community and ranges from 0 (one taxon dominates the community) to 1 (all taxa are represented equally). Berger–Parker indicates the relative abundance of the dominant OTU in each sample (for more details, see Magurran, 2004). Protistan assemblages, from the different samples, were compared using the Plymouth

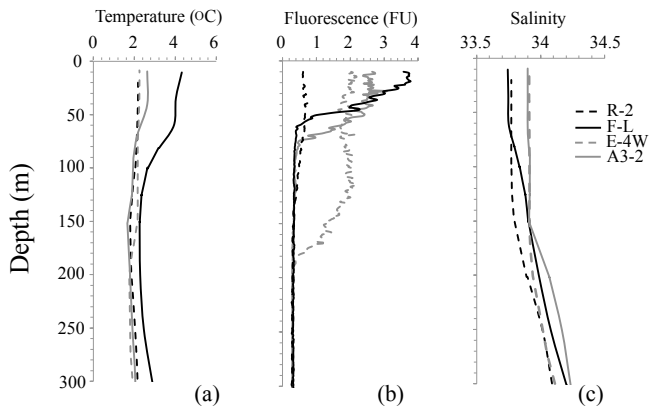


Figure 2. Profiles of temperature (a), Chl *a* as derived from in vivo fluorescence (b) and salinity (c) for each of the four sampling stations.

routines in the multivariate ecological research (PRIMER v.6) software package (Larke and Warwick, 2001). In order to identify inter-relationships between samples, Bray–Curtis similarities were analysed by cluster analysis and non-metric MDS on square-root sequence abundance. The similarity profile (SIMPROF) permutation test was conducted in PRIMER v.6 to establish the significance of dendrogram branches resulting from cluster analysis. Similarity percentage (SIMPER) analysis, also performed with PRIMER, was used to identify of the contribution of different OTUs to the observed similarity pattern.

3 Results

3.1 Study site

The hydrographic conditions during KEOPS2 are reported in detail in Park et al. (2014). The “historical” A3 station situated ~ 500 m on the Kerguelen Plateau (Blain et al., 2007, 2008) was characterized by a deep mixed layer (ML) (153 ± 15 m) (Table 1, Fig. 2). Stations F-L and E-4W revealed concentrations of 4.0 and $2.38 \mu\text{g L}^{-1}$ Chl *a*, respectively, constrained to shallow ML (38 ± 7 m and 61 ± 11 m, respectively; Table 1). The highest temperature was recorded in the ML of the F-L station (4.2 °C, Fig. 2), indicating the influence of sub-Antarctic waters. The reference site (station R-2) in HNLC waters had low concentrations of Chl *a* ($0.25 \pm 0.08 \mu\text{g L}^{-1}$), and a temperature of 2.1 °C (Fig. 2) in the ML (105 ± 15 m). The macronutrient concentrations in all 16 sampling points were high: ~ 20 – $26 \mu\text{M}$ for nitrate plus nitrite; ~ 1 – $1.8 \mu\text{M}$ for phosphate; ~ 8 – $19 \mu\text{M}$ for silicate; while dissolved iron was lower at the reference HNLC R-2 station (0.08 nM) relative to the iron-fertilized stations (0.16 – 0.22 nM; Table 2).

3.2 Composition and distribution of protistan assemblages

After quality filtering and normalization, 999 unique OTUs, clustering 50 674 sequences (average length: 240 bp) were revealed for the 16 samples. The mean ratio of observed (Table 2) to expected (S_{Chao1} , Table 2) OTUs was 75 ± 10 % (mean \pm sd) for all depths and stations. The highest number of unique OTUs, considering all depths, was observed at the F-L station (711 OTUs), and the lowest at the E-4W station (387 OTUs), while A3-2 and the HNLC R-2 stations had similar number of OTUs (550 and 496, respectively). The Simpson index was relatively high, ranging from 0.76 (F-L station in the ML) to 0.99 (HNLC, R-2 station at 300m). The Berger–Parker, indicating the relative abundance of the dominant OTU, was generally low, except at the F-L station, where it reached its highest value (0.48; Table 2).

3.2.1 High-level taxonomic groups

The 999 OTUs were affiliated into 30 higher taxonomic groups distributed in all the samples (Table 3) and shown as pie charts for each of the four stations (Fig. 3). At all stations, Alveolata was the most diverse group (696 OTUs, mainly composed of MALV-II, Dinophyceae, MALV-I and Ciliophora). The iron-fertilized stations accounted for the highest percentages of Alveolata while the lowest percentage was observed at the HNLC station R-2 (Fig. 4). Stramenopiles were represented by 133 OTUs belonging to 10 higher taxonomic groups (Table 3). The most representative Stramenopile groups, in terms of OTUs number, were MAST, followed by Bacillariophyceae and Labyrinthulomycetes (Table 3). The relative abundance of sequences of Stramenopiles ranged between 8 and 29 % in the mixed layer samples (Fig. 4). Radiolaria (belonging to Rhizaria) were present at all stations and were more abundant in the 300 m depth samples. Their relative abundance was particularly pronounced at station F-L, where they represented 55 % of all sequences (Fig. 4). The fertilized stations were characterized by lower relative abundances of Haptophyta and Chlorophyta compared with the HNLC R-2 station (Fig. 4). Fungi were represented by relatively high OTU richness (28 OTUs; Table 3). They were found almost exclusively at the fertilized stations, when only three OTUs were detected at the HNLC R-2 station (Fig. 3).

Regarding lineages distribution according to depth, the proportions of phototrophic protists (e.g. Bacillariophyceae and Haptophyta) generally decreased below the ML. The relative contribution of MALV-I and MALV-II increased with depth, at all stations except at station F-L.

3.2.2 Most abundant OTUs

The most abundant 207 OTUs, representing > 1 % of the sequences for each higher taxonomic group, accounted for 95 % of the total sequences.

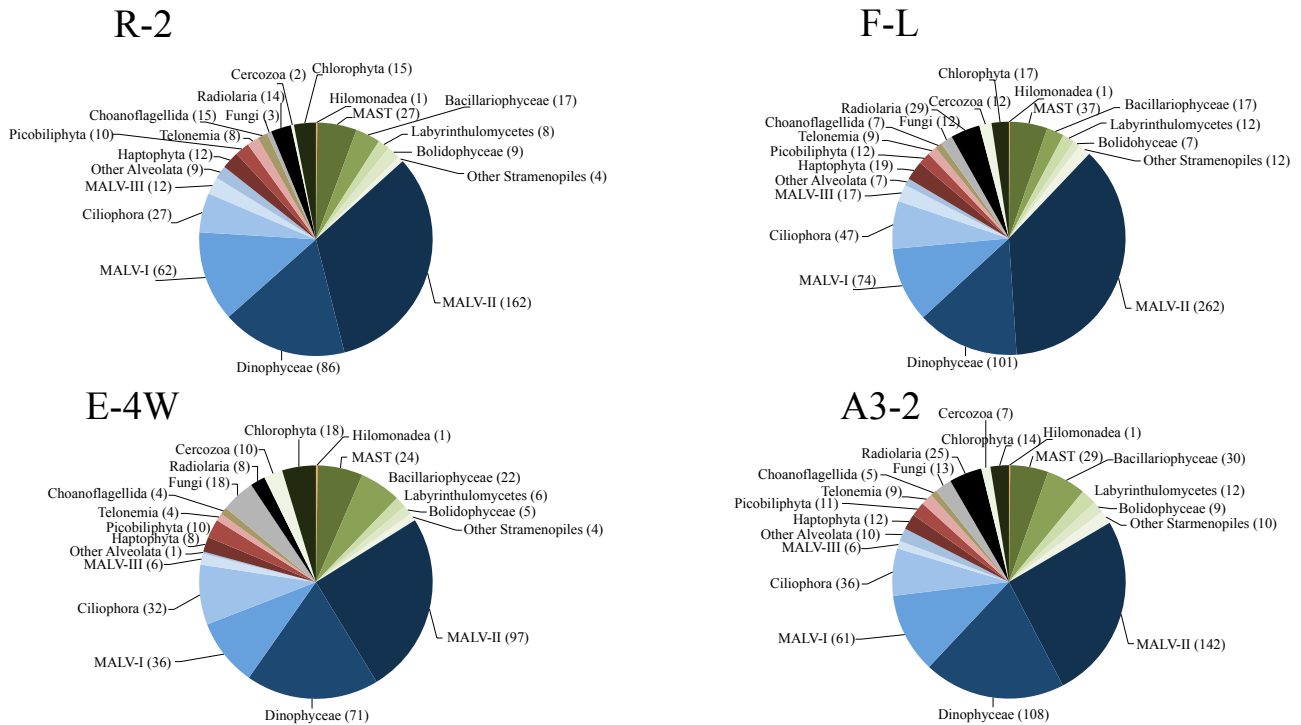


Figure 3. Overall diversity of major high-level taxonomic groups and number of OTUs indicated in parentheses at each station.

Table 2. Number of OTUs, the richness estimator (S_{chao1}), Simpson and Berger–Parker indices for each sample, number of sequences before and after removing metazoan and single singletons sequences.

Station	Depths (m)	No. OTUs	No. seqs (before)	No. seqs (after)	S_{chao1}	Simpson (1-D)	Berger–Parker
R-2	20	157	5448	4714	198	0.95	0.18
	60	170	6346	1522	218	0.95	0.16
	150	233	4407	1562	390	0.97	0.13
	300	282	1098	950	409	0.99	0.05
F-L	20	186	5586	3028	253	0.76	0.48
	65	508	7305	5730	663	0.98	0.08
	180	265	7818	905	382	0.98	0.05
	300	284	10 205	2026	383	0.83	0.40
E-4W	30	173	7151	6108	198	0.85	0.33
	80	209	10 977	6674	236	0.92	0.23
	150	191	11 989	5771	255	0.94	0.19
	300	97	3178	242	174	0.97	0.08
A3-2	320	215	10 666	1803	285	0.93	0.22
	80	200	3866	2118	273	0.98	0.08
	160	181	5986	2022	219	0.95	0.13
	300	330	11 590	5662	385	0.94	0.23

The heterotrophic *Gyrodinium* spp. was the dominant Dinophyceae genus in all samples, while the small autotrophic *Gymnodinium* spp., also present in all samples, displayed higher relative abundance in the HNLC R-2 samples (Table 4). Among Ciliophora, the genus *Strombidium* was the

most abundant, while different OTUs belonging to Tintinnid species (*Choreotrichia*) were detected at all stations. The 17 most representative MAST-related OTUs were distributed in eight clades, with a MAST-9 sp. prevailing at the surface F-L station (Table 4).

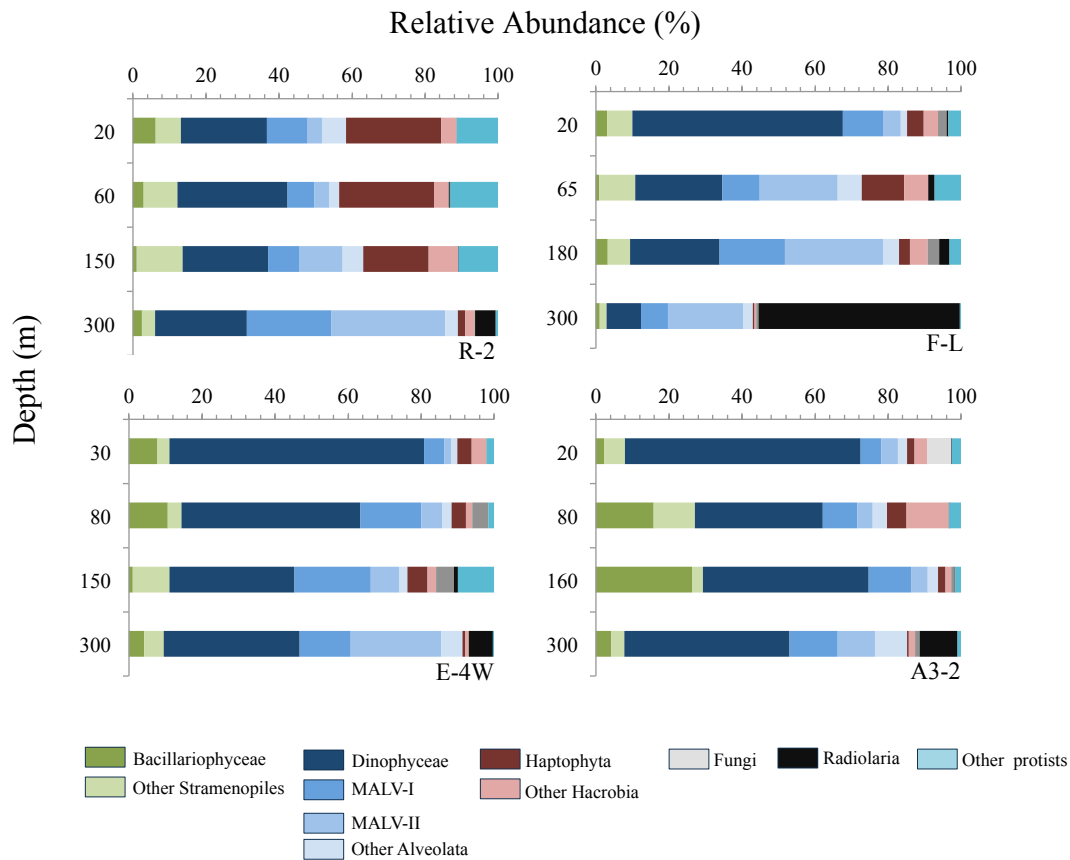


Figure 4. Relative abundance of major high-level taxonomic groups at each station and depth.

At the fertilized stations, Bacillariophyceae-related OTUs were dominated by small-sized species such as *Planktoniella*, *Thalassiosira*, and *Minidiscus* spp., while *Pseudonitzschia* was relatively abundant at the HNLC R-2 station (Table 4). Regarding the rest of the Stramenopiles, the photosynthetic picoalgae of the genus *Bolidomonas* prevailed at all stations. The non-photosynthetic Labyrinthulomycetes were more often found at the iron-fertilized stations, with the parasitic genus *Oblongichytrium* sp. being relatively more abundant at the E-4W and A3-2 stations (Table 4).

In all samples, the Haptophyta were dominated by *Phaeocystis antarctica*. Among Chlorophyta, *Micromonas* were better represented at the F-L and R-2 stations, while *Pyramimonas* spp. accounted for most of the Chlorophyta sequences at the A3-2 and E-4W stations. Choanoflagellates comprised eight OTUs, all belonging to the Stephanoecidae. Fungi were poorly represented at the HNLC R-2 station. Finally, Cercozoa were present at the iron-fertilized stations, but almost absent at the HNLC station R-2 (Table 4).

3.3 Similarity of protistan assemblages

Altogether, the stations shared 197 OTUs, with 40 OTUs specific to the fertilized stations (Fig. 5). The F-L station con-

tained the highest number of exclusive OTUs (Fig. 5). The Bray–Curtis similarity analysis of 999 OTUs indicated four major clusters (Fig. 6a). The SIMPROF significance test indicated significant differences ($P < 0.05$) between these four groups and showed significant differences within the groups (i) to (iv) (Fig. 6a). The 2-D space nMDS visual representation, based on Bray–Curtis similarity analysis, highlighted two major clusters (“shallow” and “deep” samples). An overall low similarity ($> 15\%$) was observed within each group (Fig. 6b). At a higher level of similarity (40–50%), the clusters broke roughly into individual stations: HNLC (cluster i); A3-2 (cluster ii); and E-4W (cluster iii); while the F-L 20 m and 65 m samples clustered with E-4W and the HNLC stations, respectively (Fig. 6b). Within the “deep” assemblage (cluster iv), the similarity between samples was low, except for samples R 300 m and F-L 180 m, which displayed 40% similarity (Fig. 6b). The SIMPER test highlighted the most relevant OTUs forming each cluster (Table 5). In the first cluster (i), the major contributor was Haptophyta (in particular *P. antarctica*), followed by Dinophyceae, and Chlorophyta. In the second cluster (ii), Dinophyceae contributed to 49.2% of the similarity, with *G. spirale*, having an important contribution together with 10 other Dinophyceae and Bacillariophyceae-related OTUs. In the third cluster (iii),

Table 3. Higher-level taxonomic distribution of protistan OTUs defined at 97 % sequence similarity.

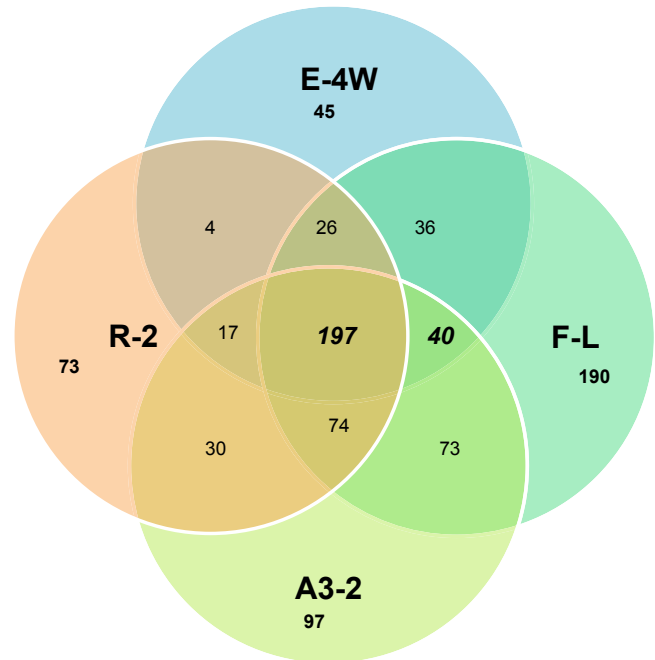
Supergroup	Taxonomic groups	OTUs
Alveolata	MALV-II	339
	Dinophyceae	161
	MALV-I	101
	Ciliophora	60
	MALV-III	21
	MALV-IV	8
	Apicomplexa	3
	MALV-V	2
	Perkinsea	1
	Stramenopiles	MAST
Bacillariophyceae		37
Labyrinthulomycetes		19
Bolidophyceae		13
Pirsonia		6
Dictyochophyceae		4
Pelagophyceae		3
Hyphochrytriaceae		2
Oomyceta		2
Chrysophyceae		1
Hacrobia		Haptophyta
	Picobiliphyta	15
	Telonemia	12
	Centroheliozoa	2
	Cryptophyta	1
Opisthokonta	Fungi	28
	Choanoflagellida	10
Rhizaria	Radiolaria	35
	Cercozoa	17
Archaeplastida	Chlorophyta	29
Apusozoa	Hilomonadea	1

Dinophyceae also prevailed (58.6 % of the similarity), with two OTUs affiliated to *G. spirale*, where *G. rubrum* was the most important. Finally, the last cluster (iv), representing the “deep” samples, was characterized by MALV-II and Radiolaria.

4 Discussion

4.1 Overview of the commonly occurring taxa according to tag pyrosequencing

This is the first broad study of protist community composition in the natural iron-fertilized Kerguelen area of the Southern Ocean. The overall taxonomic diversity of protists recovered included 999 OTUs, belonging to 30 high-level taxonomic groups. A total of 207 OTUs were classified as “abundant” (each representing ≥ 1 % of sequences in their higher

**Figure 5.** Venn diagrams representing the number of OTUs shared between the different stations.

taxonomic group) (Table 4); the most frequent OTUs belonged to Alveolata, followed by Stramenopiles, then Hacrobia (Table 3).

4.1.1 Phytoplankton

Although the tag pyrosequencing of the 18S rRNA gene has become a routine method in marine microbial diversity studies, it is itself subjected to several limitations, including, DNA extraction and PCR-related biases, chimera formation, and primer non-universality (e.g. Prokopowich et al., 2003; Ki and Han, 2005; Zhu et al., 2005; Edgcomb et al., 2011). Although it has been established that Bacillariophyceae respond to iron fertilization by rapidly forming extensive blooms (for a review see Quéguiner, 2013), concerning this study only 11 out of the 38 OTUs affiliated to Bacillariophyceae were found in common with the 52 diatom taxa morphologically identified in the Kerguelen area during the KEOPS 1 cruise at the end of the bloom period (Armand et al., 2008).

According to KEOPS2’s microscopical observations and pigment analysis data, Bacillariophyceae dominated the phytoplankton community in the blooms (Sackett et al., 2014; Lasbleiz et al., 2014). In particular, *Fragilariopsis kerguelensis*, *Pseudonitzschia* spp., *Eucampia antarctica*, and *Chaetoceros* spp. were found to be the four dominant diatom taxa, via microscopy (Sackett et al., this volume). However, while *Pseudonitzschia*-, *Eucampia*- and *Chaetoceros*-related OTUs represented 14 % of the Bacillariophyceae-related sequences, no *Fragilariopsis*-related OTUs were detected.

Table 4. Colour-coded heat-map table of the major taxonomic groups (> 10 OTUs) (see Table 3). The 207 OTUs presented here accounted for 95 % of the total sequences and represented > 1 % of sequences in each taxonomic group. The colours represent the relative abundance of each OTU within each sample. White boxes indicate absence. Black contours indicate the 17 OTUs found only at one station.

		Abs	0.1-10 %				11 to 25%				26 to 40%				41 to 60%				>60%			
OTUs	Taxonomic affiliation	Identity (%)	R-2				F-L				E-4W				A3-2							
			20m	60m	150m	300m	20m	65m	180m	300m	30m	80m	150m	300m	20m	80m	160m	300m				
MALV-II (9%)	Otu1211	Dino-Group-II-Clade0-and1 sp.	98		6.3	1.8	1.7	11.9	7.6	17.6	8.9		1.8	4.1	6.7	1.1	5.6	2.5	6.7			
	Otu1633	Dino-Group-II-Clade-5 sp.	90	36.8	6.3	1.6				1.7	1.2	16.5	19.4	9.3		3.8	1.1	28.9				
	Otu1419	Dino-Group-II-Clade0-and1 sp.	100	11.4	14.3	8.2	0.3	1.4	6.0	4.2		4.3	18.8	4.6		2.5		2.5				
	Otu1179	Dino-Group-II-Clade6 sp.	100	2.7		2.7	1.3	4.2	2.9	2.9	0.8	3.5	9.2	2.8	1.7	1.3	4.5	6.2	1.2			
	Otu1613	Dino-Group-II-Clade-7 sp.	100				5.4	0.7	12.9	4.6	1.9				3.3				3.0			
	Otu0595	Dino-Group-II-Clade-6 sp.	100		1.6	7.3	0.7	4.2	3.8	1.3	1.4	2.7		1.6		5.6	15.7	1.8	0.8			
	Otu1332	Dino-Group-II-Clade3 sp.	96		0.5	9.5	8.2		6.3	2.3	0.8	0.9	15.2	3.9								
	Otu1116	Dino-Group-II-Clade0-and1 sp.	100				2.2	9.8			0.7	4.6	0.8		1.9	15.0		1.1	1.2	8.2		
	Otu1183	Dino-Group-II-Clade-7 sp.	100					1.3			0.4	0.8			23.3				15.8			
	Otu1743	Dino-Group-II-Clade-5 sp.	92	7.3	1.6	1.6	0.7			1.7	0.4			5.6		3.8			0.4			
	Otu1926	Dino-Group-II-Clade-6 sp.	100		1.6	0.5	0.3		2.3	6.7	1.9			0.4		2.5			2.3			
	Otu1455	Dino-Group-II-Clade0-and1 sp.	100				3.2		0.7	1.9	1.3		0.9	3.9	1.9		5.6	4.8				
	Otu1947	Dino-Group-II-Clade-20 sp.	94		3.2	0.5	0.7		0.7	3.4	1.7	0.9					2.5	1.6				
	Otu1663	Dino-Group-II-Clade-7 sp.	100			1.8	3.7		0.5	0.8	3.7				11.7				2.1			
	Otu1771	Dino-Group-II-Clade-7 sp.	95				3.2		1.4	2.0			6.9		2.9							
	Otu1827	Dino-Group-II-Clade0-and1 sp.	97							2.4	0.8			1.5	1.4		8.9	5.6	2.5			
	Otu1584	Dino-Group-II-Clade-7 sp.	99					0.3		1.5	2.5	0.2				1.7	7.6		6.2	0.2		
Otu0567	Dino-Group-II sp.	93				3.8			0.6	0.4			1.7	5.5	1.9		1.1					
Otu1874	Dino-Group-II-Clade-30 sp.	98					0.7	13.9	1.1			0.2	1.7	0.8	0.3		3.4		0.2			
Otu0241	Dino-Group-II sp.	100									0.2		0.8	8.3								
Otu1468	Dino-Group-II-Clade-7 sp.	87						0.7	3.6													
Dinophyceae (40%)	Otu1951	<i>Gyrodinium spirale</i>	100	27.6	13.8	2.6	22.1	83.4	5.0	5.4	2.1	47.6	47.7	9.9		34.7	18.0	28.1	0.6			
	Otu1914	<i>Gyrodinium rubrum</i>	96	1.4	0.2	0.8		1.3	12.2	20.0		25.0	31.8	58.0		5.8	6.1	15.0				
	Otu1777	<i>Pentapharsodinium sp.</i>	97	0.9	3.7	3.3					10.0	0.8		0.7	2.2	2.1	0.7	1.8	5.7			
	Otu1967	<i>Gymnodinium sp.</i>	99	17.3	25.9	28.8	11.6	2.6	11.4	12.2	8.2	4.3	1.9	8.6	7.8	3.3	5.7	3.7	5.5			
	Otu1898	<i>Karlodinium micrum</i>	97	0.6	2.0	1.6	0.4	1.5	8.4	2.3	3.3	7.4	4.9	2.6	1.0	1.7	1.7	5.8	1.2			
	Otu1016	<i>Gyrodinium sp.</i>	98	4.9	5.3	2.2	3.4	0.7	11.6	8.6	1.7	4.0	2.4	0.8	22.2	4.5	4.2	4.3	6.5			
	Otu1770	<i>Warnowia sp.</i>	96	2.9	1.5	2.7	4.7	1.3	2.5	3.6	21.9	1.8	1.6	3.8	12.2	9.3	4.5	3.2	11.1			
	Otu1763	<i>Dinophyceae sp.</i>	100	18.2	14.5	2.7	7.2	0.7	0.7	1.4	1.6	0.4	1.1	2.7	6.7	3.5	12.2	4.8	0.3			
	Otu1808	<i>Warnowia sp.</i>	97	1.4	9.2	1.9	1.7	0.3	5.0	4.7	4.3	2.5	0.9	1.8		4.5	4.6	4.5	0.9			
	Otu1744	<i>Dinophyceae sp.</i>	100	1.3	4.8	1.6	0.4	0.2	5.6	2.7	3.3	0.8	1.0	1.7	2.2	0.3	1.4	2.3	2.3			
Otu1722	<i>Gymnodinium sp.</i>	96	0.9	1.8	2.2	0.4	0.6	5.5	2.3	1.7	1.2	1.2		2.2	1.9	2.9	1.1	0.8				
Otu1953	<i>Pentapharsodinium tyrrenicum</i>	98	0.5	2.4	3.8	6.0	0.6	3.2	3.6	1.6	0.6	1.1	0.5	4.4	1.7	1.8	2.0	1.4				
Otu1793	<i>Katodinium rotundatum</i>	95	1.3	2.0	2.0	1.3	2.6	3.4	0.9	1.6	0.8	0.6	1.9		1.9	0.7	0.7					
MALV-I (12%)	Otu1912	Dino-Group-I-Clade-1 sp.	100	4.4	7.3	9.2	6.4	5.2	11.9	8.7	0.7	24.8	31.9	28.3	2.9	16.2	16.3	11.4	11.8			
	Otu1790	Dino-Group-I-Clade-4 sp.	100	52.9	22.7	6.2	7.4	1.2	5.7	1.2	2.6	12.8	13.8	39.8	2.9	2.2		7.9	4.7			
	Otu1653	Dino-Group-I-Clade-1 sp.	100	2.6	25.5	12.4	2.9	0.7	8.3	19.3	16.3	3.8	24.6	13.7	17.6	19.2	14.8	22.3	17.5			
	Otu1285	Dino-Group-I-Clade-1 sp.	100	11.4	11.8	9.8	1.8	59.2	8.6	13.7		15.2	22.5	2.5	5.9	11.1	3.6	25.3	0.9			
	Otu1393	Dino-Group-I-Clade-1 sp.	97	1.6	10.0	6.2	0.5	1.5	22.7	3.7		2.1	0.8	3.0		6.7	2.6	0.4				
	Otu1292	Dino-Group-I-Clade-5 sp.	100		3.6	3.8	1.5		0.3	2.5	6.5		0.7	1.7	5.9	26.3	48.0	16.2	3.6			
	Otu0979	Dino-Group-I-Clade-4 sp.	100	3.9	2.7	3.8	0.5	15.6	3.0	2.5	2.6	3.9	2.6	3.2	5.9			1.7	8.6			
	Otu1753	Dino-Group-I-Clade-1 sp.	96	2.3	6.4	13.5		3.3	14.2	6.2		3.2	2.9	0.3		4.4	7.1					
Otu0518	Dino-Group-I-Clade-2 sp.	98			1.5	0.5		2.0	1.2	0.7			0.2	7.2	1.1	2.5	1.7	5.4				
Otu1920	Dino-Group-I-Clade-4 sp.	98	6.4		1.5	0.9	1.0	2.3	4.3	1.4			0.2	2.9	1.1		0.9	1.5				
Ciliophora (3%)	Otu1799	<i>Strombidium biarmatum</i>	100	26.7	25.9	28.6	21.7	26.7	34.4	25.9	2.4	34.4	44.0	6.4	15.4	2.0	32.9	13.3	7.4			
	Otu1692	<i>Strombidiidae sp.</i>	100	21.5	18.5				2.2	11.1	14.3			15.4		21.4	1.9	63.6				
	Otu1310	<i>Strombidiidae sp.</i>	100	0.8		2.6		36.7	12.4			15.6	1.7	43.6		27.5	18.6	15.9				
	Otu1672	<i>Choreotrichia sp.</i>	98			1.6	13.4		1.9	3.7	2.4		0.7	14.1	23.8	5.0	2.9	13.3	11.7			
	Otu0922	<i>Pelagostrombidium neptuni</i>	99	14.4		1.6		6.7	0.7			4.2	2.0					5.7				
	Otu1845	<i>Choreotrichia sp.</i>	95	2.3		1.6	4.3	3.3	8.3				0.7			5.0			28.3			
	Otu1773	<i>Laboea strobila</i>	97	4.3	29.6			3.3	0.4			9.4	11.3									
	Otu0371	<i>Cymatocylis calyciformis</i>	100	1.6				3.3					12.0					1.4				
	Otu1018	<i>Strombidium caudatum</i>	96	1.1	3.7				1.5	7.5		3.1		1.3		2.5	5.7					
	Otu1467	<i>Pseudotontonia sp.</i>	100	2.7	11.1	3.2		3.3			2.4	14.6	2.0			12.5	2.9	1.9				
	Otu0336	<i>Collinia beringensis</i>	98								7.1			28.3					1.9			
	Otu1053	<i>Mesodiniidae sp.</i>	98			1.6	34.8		1.9	3.7	4.0				7.7				0.5			
	Otu0145	<i>Pseudotontonia simplicidens</i>	100	2.7					2.2			6.3	4.7			2.5						
	Otu1601	<i>Scuticocliatia sp.</i>	97				8.7		1.9		7.1					2.5			2.9			
	Otu1320	<i>Choreotrichia sp.</i>	93						4.4	3.7				2.8	0.7	2.5	2.9	1.9				
	Otu0516	<i>Mesodiniidae sp.</i>	89			1.6			2.6					0.7					2.4			
	Otu1317	<i>Colpodea sp.</i>	87			7.9			2.2	3.7				3.1	0.7							
Otu1614	<i>Strombidiidae sp.</i>	99						4.4		2.4							5.7					
Otu1322	<i>Strombidium basimorphum</i>	98						5.2	3.7						2.5							
MALV-III (0.5%)	Otu1426	Dino-Group-III sp.	100		20.0	81.8	27.3	50.0		21.5	33.3		6.7				72.7		16.7			
	Otu1030	Dino-Group-III sp.	95		26.0		18.2		13.9	11.1			36.4	100.0		20.0		100.0				
	Otu1731	Dino-Group-III sp.	95		10.0	18.2	18.2		5.6	22.8	11.1		13.3									
	Otu1911	Dino-Group-III sp.	95		30.0		9.1		5.6	2.5	11.1											
	Otu0008	Dino-Group-III sp.	93						1.3					66.7		60.0	27.3					
	Otu1429	Dino-Group-III sp.	93						83.3													
	Otu1958	Dino-Group-III sp.	99		2.0					15.2												
	Otu1093	Dino-Group-III sp.	89			4.5			5.6	7.6	11.1											
	Otu1664	Dino-Group-III sp.	89				9.1				11.1				13.3							

Table 4. Continued.

MAST (4%)	Otu1762	MAST-1B sp.	100	2.4	15.3	27.7	1.0	24.3	25.7	23.8	9.5	6.0	9.2	1.2	33.3	9.4	15.5	2.4	3.6	
	Otu1923	MASTC sp.	100	17.2	2.3	16.8	15.0	6.4	1.7	7.7	9.5	12.0	6.2	8.8		4.8	7.2	11.9	4.8	
	Otu0923	MAST-8 sp.	100	1.3	3.4	19.8		2.3	6.0	2.6		3.6	3.8	17.3		4.8	5.2	9.5	23.9	
	Otu1031	MAST-1C sp.	100	1.3	8.5	1.0	1.0	2.3	9.1	7.7			4.6	11.9		22.4	5.7	21.4	2.4	
	Otu0641	MAST-3 sp.	84					4.6	1.0			13.8	1.0	13.8		7.6	16.5	4.8		
	Otu1618	MAST-9 sp.	99	2.0					0.7	7.7	4.8			18.5	2.4			16.7	3.6	
	Otu0656	MAST-2 sp.	100	12.5	6.8	1.0		1.2	2.4		9.5	28.1	19.2			4.8	3.7			
	Otu1009	MAST-1A sp.	100	5.9	1.2	7.9	15.0	2.3	8.2	2.6		5.4	6.2	0.5		4.8	9.3		6.0	
	Otu1638	MAST-9 sp.	97					42.8	0.5	5.1				6.9				7.1		
	Otu1205	MAST-7 sp.	100	0.7	3.4	5.9		1.2	3.6	5.1	4.8	4.2	0.8	0.5		12.9	9.8	9.5	9.5	
	Otu1908	MAST-3 sp.	95	2.0	5.8	1.0			5.5	5.1		9.0	3.8	3.3		4.8	5.7	2.4		
	Otu1788	MAST-3 sp.	96	3.9	11.9	4.0			1.2	5.1		3.6	5.4	9.3		1.2	1.4			
	Otu1235	MAST-7 sp.	98	1.3				4.6	6.7			1.2	4.6			8.2	9.3	2.4		
	Otu0973	MAST-1A sp.	100	17.2	1.7			1.7	2.9			3.6		0.2			1.5		4.8	
	Otu1208	MAST-7 sp.	96	3.9	5.8	10.0		1.2	3.4			3.6		0.7		4.8	3.7			
	Otu1567	MAST-3 sp.	95	9.9			5.0	1.2	1.0	5.1	4.8	3.0							4.8	
	Otu1546	MAST-3 sp.	87						1.7		4.8	0.6	0.8	0.7		5.9	2.6	11.9	2.4	
Bacillariophyceae (6%)	Otu1447	<i>Planktoniella</i> sp.	100	3.9	25.6	11.8	22.7	42.6	18.5	24.1	57.1	6.3	29.8	23.7	4.0	39.0	51.5	35.7	42.3	
	Otu1564	<i>Coccinodiscus triculatus</i>	100		2.3	5.9		47.9	24.7	2.7	19.5	11.4	16.9			9.5	1.2	0.2	5.3	
	Otu0904	<i>Coccinodiscus</i> sp.	95									15.4	16.8	27.1	2.0	19.5	1.0		13.0	
	Otu0581	<i>Rhizosolenia styliformis</i>	100					2.1			4.8	4.8	0.4	16.9		2.4	6.7	32.9	2.5	
	Otu1786	<i>Pseudo-nitzschia pungens</i>	100	52.6	37.3		22.7		1.9				1.7		2.0		2.7	4.7	2.9	
	Otu1293	<i>Corethron pennatum</i>	95	8.3	9.3	5.9			1.9			2.8	18.0	1.7	1.0	4.8	1.2	0.8	3.3	
	Otu0978	<i>Thalassiosira delicatula</i>	100					1.6		3.4		0.4	0.3			4.8	24.9	16.3		
	Otu1787	<i>Actinocyclus actinochilus</i>	99	14.9	14.0	35.3	13.6						1.9		1.0	4.8	1.5	0.2	8.8	
	Otu1372	<i>Pseudo-nitzschia multiseriis</i>	99	16.3	7.0		13.6		1.9			0.6				4.8		1.3		
	Otu0005	<i>Thalassionema nitzschoides</i>	100										1.3	18.6		2.4	1.8	0.4	8.4	
	Otu0184	<i>Guinardia flaccida</i>	92										3.6	11.9						
	Otu1536	<i>Eucampia antarctica</i>	100		29.4	22.7			1.9		4.8						0.3	0.4		
	Otu0756	<i>Porosira pseudodenticulata</i>	100						11.1	31.0	14.3									
	Labyrinthulomycetes (0.7%)	Otu0727	<i>Oblongichytrium</i> sp.	90		14.3			18.2	6.0	11.1	20.0				72.1	87.2	88.9		13.2
Otu0512		<i>Labyrinthulaceae</i> sp.	92	16.7				45.5	30.0	11.1	26.7				8.2	6.4	11.1	100.0	68.8	
Otu0042		<i>Labyrinthulaceae</i> sp.	100			50.0			26.0	55.6	13.3								25.0	
Otu0984		<i>Labyrinthulaceae</i> sp.	88	33.3	85.7			4.5	16.0			100.0	3.3					6.3	25.0	
Otu1330		<i>Oblongichytrium</i> sp.	91										14.8	5.5					2.6	
Otu0193		<i>Oblongichytrium</i> sp.	92						16.0	11.1	13.3									
Otu1747		<i>Labyrinthulaceae</i> sp.	90				25.0												5.3	
Otu0468		<i>Oblongichytrium</i> sp.	91					27.3												
Otu0253		<i>Labyrinthulaceae</i> sp.	94										1.6				12.5	50.0		
Otu0717		<i>Oblongichytrium</i> sp.	90		16.7						11.1	6.7			0.9					
Bolidophyceae (3.1%)	Otu1213	<i>Bolidophyceae</i> sp.	99	30.8	33.3	12.5		25.0	33.3			80.8	68.2	52.0		72.7	84.6	80.0	89.3	
	Otu1903	<i>Bolidomonas mediterranea</i>	90	30.8	13.3	87.5		52.8				3.8	29.5	44.0			3.8			
	Otu0192	<i>Bolidophyceae</i> sp.	93	28.2	20.0															
	Otu1883	<i>Bolidophyceae</i> sp.	90			66.7	80.0	5.6	66.7										5.4	
	Otu0147	<i>Bolidomonas mediterranea</i>	95	10.3					2.8					4.0	100.0	18.2	3.8	20.0		
	Otu0624	<i>Bolidomonas pacifica</i>	97		20.0			20.0	8.3							9.1				
	Otu0016	<i>Bolidophyceae</i> sp.	88									15.4					3.8			
	Otu1713	<i>Bolidomonas mediterranea</i>	90		6.7				2.8				2.3				3.8			
	Haptophyta (7%)	Otu1782	<i>Phaeocystis antarctica</i>	100	67.3	62.8	71.2	58.8	78.7	66.6	53.3		69.7	65.2	66.2	1.0	62.2	62.3	87.8	9.0
		Otu1907	<i>Chrysochromulina strobilus</i>	100	5.2	1.7	9.3	11.8	11.3	11.7	13.3	14.3	2.9	26.2	25.6		18.9	9.6	7.3	
Otu1884		<i>Chrysochromulina</i> sp.	97	11.6	19.8	17.4	5.9	9.6	1.8		14.3	6.0	3.3				1.5	4.9		
Otu1778		<i>Gephyrocapsa oceanica</i>	100	13.1	3.5		17.6		3.0	3.3						5.5				
Otu1026		<i>E. anthemachrysis gayraliae</i>	93	0.2	0.8	1.7			2.2			3.4	5.3	0.3		2.7	6.1		3.3	
Otu1774		<i>Chrysochromulina hirta</i>	100	1.0	1.2		5.9	0.7	1.2		57.1			3.6			0.9			
Picobiliphyta (3.1%)		Otu1423	Picobiliphyta sp.	94	57.0	16.7	33.3	4.5	6.8	25.6	32.5	50.0	29.6	11.8	23.1		24.1	27.9	21.4	5.0
	Otu1067	Picobiliphyta sp.	100		7.1	21.6		43.6	17.9	17.5	16.7	18.5	26.9	1.5		14.8	25.0	3.6	18.3	
	Otu1965	Picobiliphyta sp.	99	4.7	14.3	17.1	40.9	18.8	8.2	12.5		12.0	14.0	45.5		9.3	11.7	25.0	13.3	
	Otu1899	Picobiliphyta sp.	99		2.4	2.7		17.1	21.2	5.0		15.0	12.9	0.7		11.1	10.4	14.3		
	Otu1387	Picobiliphyta sp.	96	17.4	21.4	9.9	22.7	0.9	5.3	12.5		6.9	22.6	17.9		16.7	8.8	14.3	5.0	
	Otu1025	Picobiliphyta sp.	92	20.9	28.6	6.3	4.5	0.9	6.2			5.2	4.3			9.3	3.3	3.6	35.0	
	Otu1275	Picobiliphyta sp.	94		4.8	5.4		8.5	4.1	10.0		4.7	3.2	9.7		3.7	0.4	7.1	18.3	
	Otu1283	Picobiliphyta sp.	100		4.8	2.7		2.6	6.5			3.4	4.3	1.5		9.3	6.7	3.6		
	Otu1792	Picobiliphyta sp.	100				27.3	0.9	4.1	7.5	16.7	3.9				1.9	4.6	7.1	5.0	
Telonemia (0.5%)	Otu1780	Telonemia-Group-1 sp.	97	57.8	66.7	7.1		25.0	16.7			93.3	42.9		12.5	33.3	33.3			
	Otu0011	Telonemia-Group-2 sp.	100	16.5				50.0	30.0	75.0			57.1		25.0	66.7				
	Otu1445	Telonemia-Group-2 sp.	97	13.8	13.3	28.6		25.0	13.3			6.7			12.5					
	Otu1575	Telonemia-Group-2 sp.	98							25.0	50.0								51.3	
	Otu0345	Telonemia-Group-2 sp.	100	8.3	13.3	42.9			10.0										0.0	
	Otu0040	Telonemia-Group-2 sp.	97			7.1	50.0												38.5	
	Otu0585	Telonemia-Group-1 sp.	99	3.7	6.7	7.1			16.7							25.0				
	Otu0140	Telonemia-Group-2 sp.	97			7.1			6.7							25.0			33.3	
	Otu0075	Telonemia-Group-2 sp.	100																10.3	
	Otu0732	Telonemia-Group-2 sp.	97				50.0		6.7										33.3	
Fungi (2%)	Otu1863	<i>Exobasidiomycetes</i> sp.	100		83.3		100.0	66.7		6.7	15.4	1.0	29.6	5.0		89.2		52.4	7.4	
	Otu0879	<i>Candida austromarina</i>	100										17.9	3.3						
	Otu1430	<i>Laccocephalum mylittae</i>	88					12.5					8.2	1.7						
	Otu0716	<i>E. obasidiomycetes</i> sp.	100					12.5					13.6			5.0		4.8		
	Otu1424	<i>Coccodinium bart</i>																		

Table 4. Continued.

Choanoflagellida (1%)	Otu1941	StephanoecidaeGroupD sp.	97	22.2	10.0	11.1	25.0	33.3	44.1	25.0	63.3	4.0	21.5	73.3	66.7	4.0	25.0		
	Otu1928	Stephanoeca cauliculata	99	57.5	72.7	55.6	25.0	11.8	25.0	16.7	1.0	1.8	13.3	16.7	6.0	25.0			
	Otu1710	StephanoecidaeGroupD sp.	100	18.5	18.2			23.5		66.7	5.0	43.8	6.7	13.3		25.0			
	Otu0960	StephanoecidaeGroupH sp.	90					66.7	2.9	25.0		24.6							
	Otu1959	StephanoecidaeGroupD sp.	95			11.1		11.8						3.3		25.0			
	Otu1706	StephanoecidaeGroupD sp.	93	1.9						25.0	33.3			6.7					
	Otu1905	StephanoecidaeGroupH sp.	91			22.2													
	Otu1828	StephanoecidaeGroupD sp.	94				5.0												
Radiolaria (4%)	Otu1699	Spumellarida-Group-I sp.	99			67.9		4.2	8.0	73.7			18.8			50.7			
	Otu1655	Spumellarida-Group-I sp.	100					16.7	1.1	4.0	13.9					1.0			
	Otu1138	<i>Stylocditya</i> sp.	99			1.9	25.0	42.1	16.0	0.4		37.5	33.3			7.7			
	Otu1589	Spumellarida-Group-I sp.	100						4.0	6.7						0.3			
	Otu0699	<i>Triastrum aurivillii</i>	95	25.0				1.1				76.2				1.7			
	Otu1856	RAD-B-Group-IV sp.	99		50.0	1.9		12.6	8.0	0.3		6.3	33.3		66.7	5.8			
	Otu0036	RAD-B-Group-IV sp.	97			1.9			8.0							7.5			
	Otu0686	RAD-B-Group-II sp.	100													7.4			
	Otu1654	RAD-B-Group-II sp.	99			5.7		2.1	4.0							5.8			
	Otu1349	RAD-B-Group-IV sp.	100	75.0				17.9	16.0			19.0		100.0	33.3				
Cercozoa (1%)	Otu1449	<i>Protocystis iphodon</i>	100					2.6											
	Otu1378	<i>Protospa-lineage</i> sp.	98			100.0		30.8	26.7		6.7			33.3	28.6	33.3	100.0		
	Otu1257	<i>Ebria tripartita</i>	100					51.3	20.0										
	Otu0591	<i>Protospa-lineage</i> sp.	99					2.6	6.7		46.7	13.3							
	Otu0887	<i>TAGIRI1-lineage</i> sp.	98									40.0			28.6				
	Otu1806	<i>Protospa</i> sp.	99			100.0		10.3						16.7					
	Otu0881	<i>Cryothecomonas-lineage</i> sp.	99										33.3						
	Otu0170	<i>Cryothecomonas-lineage</i> sp.	100						6.7					33.3		33.3			
	Otu0742	<i>TAGIRI1-lineage</i> sp.	98									13.3		16.7	14.3				
	Otu0201	<i>Cryothecomonas</i> sp.	100					20.0											
	Otu1040	<i>Matoza-lineage</i> sp.	100					2.6				13.3							
	Otu1368	<i>Protospa-lineage</i> sp.	100						6.7							33.3			
	Otu0857	<i>Cryothecomonas</i> sp.	99									13.3							
	Otu0941	<i>Marimonadida</i> sp.	92									13.3							
Otu1624	<i>Endo4-lineage</i> sp.	99								100.0									
Chlorophyta (4%)	Otu1717	<i>Micromonas pusilla</i> (RCC658)	100	2.0	28.8	3.5		25.4	38.6	68.4		1.0	6.6	5.2		5.9	3.3		
	Otu1962	<i>Pyramimonas gelidicola</i>	97	6.9	4.0	2.3			0.9			1.8	72.5	29.6		17.4	2.9	53.3	
	Otu1742	<i>Micromonas pusilla</i> (RCC418)	100	22.7	29.9	3.5		13.6	21.6	5.3		30.0	6.1				3.3		
	Otu1918	<i>Bathycoccus prasinos</i>	100	12.8	26.6	34.5		6.8	16.5			10.0	4.4	1.0		17.6			
	Otu1791	<i>Prasinoderma coloniale</i>	95	33.5	3.4		5.0	8.5	2.5	15.8			0.9	3.8			3.3		
	Otu0166	<i>Pyramimonas disomata</i>	96	2.7	1.1		5.0							33.3			6.7		
	Otu1766	<i>Pyramimonas olivacea</i>	99	2.2	1.7	1.4		3.4	2.2		1.0	5.5		18.5		47.8	14.8	6.7	48.3
	Otu0940	<i>Pyramimonas</i> sp.	100		0.6	0.7		1.2	1.5			13.6	4.4	4.6		13.4	41.2	1.0	
	Otu1775	<i>Crustomastigaceae</i> sp.	99	0.2				16.9	0.4	5.3		10.0	1.3	3.6		17.6		51.7	
	Otu0151	<i>Mamiella</i> sp.	100			0.7		6.7	2.5			6.3	1.7			4.3			

Potential limitation regarding pyrosequencing detection of Bacillariophyceae have been reported recently in an extensive study at the San Pedro Ocean Time Series station (SPOT, Lie et al., 2013). They can be related to extraction efficiency from thick walled diatoms (Medinger et al., 2010) and/or amplification biases favouring species with high 18S rRNA gene copy number, such as ciliates and dinoflagellates (Potvin and Lovejoy, 2009). It is also worth noting that 28 out of the 52 taxa identified by microscopy (Armand et al., 2008) were not referenced in the GenBank. Finally, regarding the 27 diatom taxa that were “identified” only by pyrosequencing – based on sequence similarity with the closest existing cultured relatives in GenBank – they mainly belonged to the genera previously observed in this area (Armand et al., 2008). The accuracy of BLAST-derived taxonomy, especially at low-level taxa, depends on sequence length, variability of the 18S region, database coverage for the specific taxonomic group, and correct identification of the reference sequence (Bik et al., 2012).

Sequences belonging to the nano- and picophytoplanktonic groups of Bolidophyceae, Pelagophyceae,

Chrysophyceae and Cryptophyta were found at relatively low abundances in all samples. Moreover, Haptophyta were dominated by an OTU affiliated as *Phaeocystis antarctica* (100% sequence identity). This phylotype has been previously reported as dominant in the south of the polar front (Wolf et al., 2014), in the Ross Sea waters (DiTullio et al., 2000), and in the naturally iron-fertilized bloom around the Crozet Plateau (Poulton et al., 2007).

4.1.2 Microzooplankton: Dinoflagellates, ciliates and radiolaria

Although Dinophyceae might be over-represented in the sequence data, possibly due to its high 18S gene copy number (e.g. Prokopowich et al., 2003; Zhu et al., 2005), tag pyrosequencing has made possible the highlighting of its extensive diversity (161 OTUs) in the Southern Ocean – previously missed by conventional microscopy and/or pigment analysis (see also Wolf et al., 2014). For example, based on microscopy, *Gyrodinium* is the most abundant dinoflagellate analysed; however, no reliable distinction has been made

Table 5. Results of SIMPER (similarity percentages) following the Bray–Curtis cluster analysis (Fig. 6a). Forty-one OTUs contributing for at least 1 % of the similarity of each cluster are listed in this table. In parentheses, the mean of Bray–Curtis similarity is given for each cluster.

OTUs	Taxonomic groups	Putative taxonomic affiliation	Cluster (i) (43.8 %)	Cluster (ii) (51.8 %)	Cluster (iii) (47.6 %)	Cluster (iv) (20.7 %)
Otu1951	Dinophyceae	<i>Gyrodinium spirale</i>	5.1	17	33.5	1.3
Otu1914		<i>Gyrodinium rubrum</i>		5.2	17.9	
Otu1967		<i>Gymnodinium</i> sp.	8.8	3.5	2.6	4.9
Otu1898		<i>Karlodinium micrum</i>		5.9	1.9	1.3
Otu1770		<i>Warnowia</i> sp.		3	1.5	4.1
Otu1016		<i>Gyrodinium rubrum</i>	1.3	3.3		3.6
Otu1763		<i>Dinophyceae</i> sp.	1.5	3.7		1.5
Otu1808		<i>Warnowia</i> sp.	1.8	3.6		
Otu1953		<i>Peridinium tyrrhenicum</i>		1.4		1.8
Otu1871		<i>Gymnodinium catenatum</i>				1.7
Otu1816		<i>Karlodinium micrum</i>				1.3
Otu1722		<i>Gymnodinium</i> sp.		1.3		
Otu1454		<i>Islandinium minutum</i>		1.3		
Otu1793		<i>Amphidinium semilunatum</i>			1.1	
Total				18.4	49.2	58.6
Otu1653	MALV-I	Dino-Group-I-Clade-1 sp.	1.3	2.2	2.1	6
Otu1912		Dino-Group-I-Clade-1 sp.		1.9	3.2	1.4
Otu1292		Dino-Group-I-Clade-5 sp.		2.9		1.6
Otu1285		Dino-Group-I-Clade-1 sp.	1.3		2.6	
Otu1790		Dino-Group-I-Clade-4 sp.	1.2		1.4	
Otu1393		Dino-Group-I-Clade-1 sp.	1			
Total				4.7	6.9	9.2
Otu1211	MALV-2	Dino-Group-II-Clade-10 sp.				3.7
Otu1116		Dino-Group-II-Clade-10 sp.				3.2
Otu1663		Dino-Group-II-Clade-7 sp.				2
Otu1613		Dino-Group-II-Clade-7 sp.				2
Otu1513		Dino-Group-II-Clade-6 sp.				1.1
Otu1183		Dino-Group-II-Clade-7 sp.				1.1
Total						13.1
Otu1799	Ciliophora	<i>Strombidium biarmatum</i>	1.2			
Otu1447	Bacillariophyceae	<i>Thalassiosira tenera</i>		6.4	2	1.9
Otu0978		<i>Thalassiosira delicatula</i>		2.7		
Total				9.1	2	1.9
Otu1932	Pelagophyceae	<i>Aureococcus anophagefferens</i>	4.7			
Otu1762	MAST	MAST-1B sp.	1.3			
Otu1923		MAST-1C sp.	1.1			
Total			2.4			
Otu1717	Chlorophyta	<i>Micromonas pusilla</i>	4			
Otu1918		<i>Bathycoccus prasinos</i>	3.8			
Otu1742		<i>Micromonas pusilla</i>	3.8			
Total			11.5			
Otu1782	Haptophyta	<i>Phaeocystis antarctica</i>	18.3	2.7	5.2	1.3
Otu1884		<i>Chrysochromulina strobilus</i>	4.5			
Otu1907		<i>Chrysochromulina</i> sp.	2.7		1.3	
Total			25.5	2.7	6.4	1.3
Otu1863	Fungi	<i>Malassezia restricta</i>	1.3			
Otu1699	Radiolaria	<i>Spumellarida</i> sp.				6.2
Otu1138		<i>Stylodictya</i> sp.				1
Total						7.2

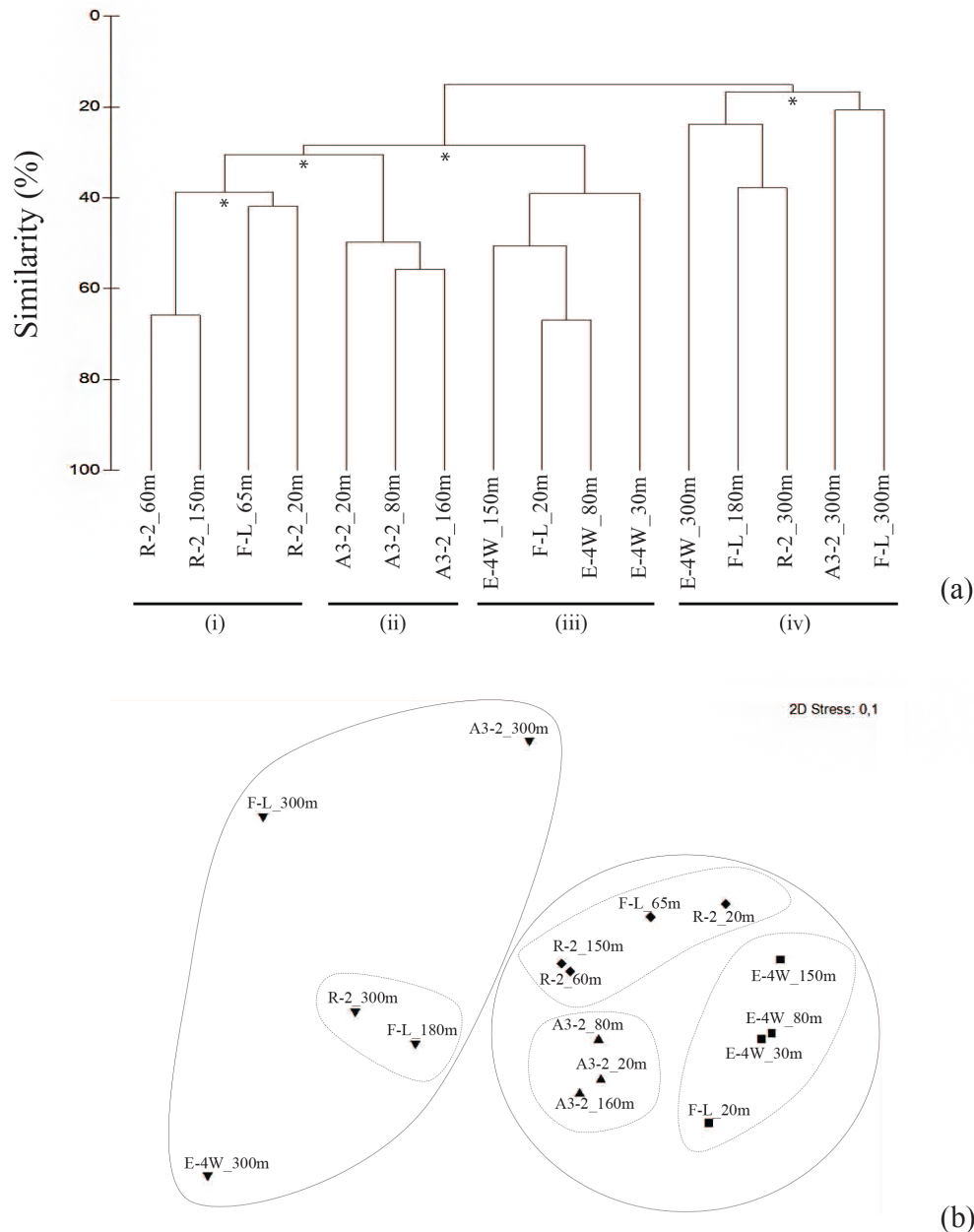


Figure 6. Cluster diagram for the 16 samples constructed from a Bray–Curtis similarity matrix of square-root-transformed OTU abundances. Asterisks at nodes in the dendrogram indicate significant differences between bifurcations ($P < 0.05$) (a). Nonmetric multidimensional (nMDS) scaling plots in two dimensions constructed from a Bray–Curtis similarity matrix. Bray–Curtis similarity contours are 15 % (solid lines) and 40 % (dashed lines) (b).

between *G. spirale* and *G. rubrum* with morphological observations (Saito et al., 2005; Georges et al., unpublished KEOPS2 data)

Ciliophora, which are ecologically important grazers of small-sized phytoplankton, accounted for a relative high number of OTUs (60 OTUs). As with previous microscopic observations in the Kerguelen area (Christaki et al., 2008), the most representative ciliate sequences in this study belonged to Strombidiidae. The relatively large-sized *Strom-*

bidium spp. ($\geq 50 \mu\text{m}$) can be plastidic (mixotrophic) and along with *Tontonia* spp. and *Laboea* spp. – also present in sequences – were found to contribute to 40–60 % of the aloricate ciliate biomass during the late bloom on the Kerguelen plateau (KEOPS1, Christaki et al., 2008). Finally, the most relatively abundant sequences of tintinnid taxa – which are also important nanophytoplankton consumers – belonged to the large *Cymatocyclis calyciformis* (Christaki et al., 2008).

Radiolaria were another well-represented microzooplankton group (35 OTUs). These can act as particle feeders, by trapping their prey on the peripheral network of rhizopodia, or capture diatoms. They are also hosts of dinoflagellate symbionts and parasites, and may be important reservoirs of MALV taxa (e.g. Bråte et al., 2012). In this study, the relative increase of MALV with depth was consistent with a parallel increase of Radiolaria. This observation is also supported by the hypothesis that MALV taxa are able to parasitize “deeper” planktonic organisms such as Spumellarida (Guillou et al., 2008), which were the most common group and were always well represented in the deeper water samples in this study (Fig. 4, Table 4). Radiolaria and MALV taxa characterizing deeper protistan assemblages have also been reported in the North Atlantic (Countway et al., 2007; 2010; Not et al., 2007) and deep Antarctic polar front samples (López-García et al., 2001).

4.1.3 Symbionts, parasites, and decomposers

This assemblage included the taxonomic groups of MALV-I, MALV-II, Labyrinthulomycetes, Pirsonia, Oomyeta, Apicomplexa, Perkinsea, Fungi and Cercozoa. Many of these groups have a zooflagellate stage in their life cycles, and are classified together in microscopical studies as “heterotrophic nanoflagellates”. MALV-I and MALV-II appear in virtually all marine surveys (López-García et al., 2001; Massana and Pedrós-Alió, 2008). Their considerable abundance and diversity suggests interactions with various hosts, and therefore it has been proposed that the whole MALV assemblage is composed of marine parasites (Skovgaard et al., 2005; Massana and Pedrós-Alió, 2008).

Fungi and Cercozoa accounted for 28 and 17 OTUs, respectively. In a recent succession study in the English Channel, it was observed that these groups mostly co-occurred with Bacillariophyceae (Christaki et al., 2014). Fungi are possibly related to the polysaccharide degradation of the freshly produced organic material by primary producers (Kimura and Naganuma 2001; Raghukumar, 2004). It is known for diatoms that polysaccharides are their main exudates (Myklestad, 1995 and references therein), and these sugars could promote the growth of Fungi. Many Cercozoa are parasites of marine organisms, including large heavily silicified diatoms (e.g. Tillman et al., 1999; Schnepf and Kühn, 2000), which could explain why Fungi and Cercozoa were detected in the bloom stations and were poorly represented (2–3 OTUs, Table 4) at the HNLC R-2 station. Labyrinthulomycetes were also better represented in terms of numbers of sequences in the bloom stations (Table 4). Labyrinthulomycetes (19 OTUs) are common osmo-heterotrophic marine protists (López-García et al., 2001) having parasitic, commensalistic, or mutualistic relationships with their hosts.

They play an important role in decomposition processes (Collado-Mercado et al., 2010) by colonizing fecal pellets, including under deep-sea conditions (Raghukumar, 2004).

4.1.4 Small heterotrophic protists

Among the small heterotrophic protists found in the samples, there were a variety of MAST (46 OTUs), Choanoflagellida (10 OTUs) and Telonemia (12 OTUs). MAST taxa are widely distributed in the world’s oceans, and have been identified as free-living bacterivorous heterotrophic flagellates through a combination of FISH and other measurements (Massana et al., 2006; Jürgens and Massana, 2008 for a review). Choanoflagellida of the genus *Stephanotheca* sp. were also observed by epifluorescence microscopy in KEOPS2 samples, and were more abundant and diversified in the 0–200 m layer (Georges et al., unpublished KEOPS2 data).

4.2 Variability of protistan assemblages relative to iron fertilization

In general, the stability of OTUs richness and diversity indices between the HNLC R-2 and iron-fertilized stations indicated that the environment maintained an overall diversity across stations and depths (Table 2). These observations are in agreement with previous molecular studies based on protistan diversity (e.g. Countway et al., 2007; Monchy et al., 2012). However, community structure analysis showed clear differences inside and outside the blooms (Fig. 6a).

4.2.1 HNLC station

Based on trophic organization, HNLC areas seem conceptually similar to oligotrophic regions dominated by small producers and an active microbial food web (e.g. Hall and Safi, 2001; Oliver et al., 2004; Christaki et al., 2014, 2008; Obernosterer et al., 2008). The characteristic contributors of the HNLC cluster (i) were Haptophyta, Chlorophyta and MAST, which included mainly nanoplanktonic organisms. During KEOPS2, the relative importance of small-sized cells at the HNLC station is in accordance with the flow cytometry data ($4.8 \pm 1.9 \cdot 10^3 \text{ mL}^{-1}$ nano-picophytoplankton cells in comparison to $1.8 \pm 1.3 \cdot 10^3 \text{ mL}^{-1}$ at the bloom stations; KEOPS2 data). The factors influencing phytoplankton community composition (e.g. diatoms vs. *Phaeocystis* sp.) in the Southern Ocean are a complex interplay between bottom-up (iron–silicate–light availability; controlling growth) and top-down effects (grazing; controlling mortality) (Cullen, 1991; Arrigo et al., 1999; Smetacek et al., 2004; Schoemann et al., 2005). Live plankton observations completed on board (<https://www.youtube.com/watch?v=KPgoz8bWRJU>) revealed the presence of small colonies and free-living cells belonging to the Haptophyta *Phaeocystis* sp. at all stations. It seems that *Phaeocystis* species cope best with the environmental conditions in the open ocean waters south of the Polar

Front, where it was found to be the most dominant phylotype (Wolf et al., 2014).

4.2.2 Iron-fertilized sites

The mechanisms that fertilize the surface water in the region around Kerguelen are complex, which results in a patchwork of blooms with diverse biological and biogeochemical response. The phytoplankton bloom at the “historical” A3 station situated on the Kerguelen Plateau is bottom-up sustained by low-level supplies of iron and other nutrients (Blain et al., 2007). Drifters have revealed a northeastward-driven circulation pattern in the Kerguelen Plateau and oceanic area, while strong horizontal mixing have been found in the East Kerguelen Basin off the plateau (Zhou et al., 2014; Fig. 1b). Station E-4W is located at the shelf break in a region with very strong currents (Zhou et al., 2014), and consequently receives iron-rich waters from the Kerguelen Island and Plateau (A3 station area) which mix with Polar Front waters that cross the Kerguelen Plateau while traveling northeast (Fig. 1b). The depth of the ML varied considerably, from 40 m north of the Polar Front at station F-L to 170 m above the plateau at station A3. In accordance with these hydrographic characteristics, multivariate analysis of sequences showed that the ML sample of the F-L (20 m) was found in the same cluster as the E-4W samples, while the 65 m F-L sample was grouped with the HNLC samples. The OTUs putatively affiliated to heterotrophic dinoflagellate taxa (Table 5) were the major contributors of clusters (ii) and (iii) (Fig. 6a, b). Dinoflagellate increase during iron-fertilized blooms – in particular, *Gyrodinium* spp. has been observed with microscopic counts during the iron addition experiments, and has been attributed to the increase of their diatoms prey (Hall and Safi, 2001; Saito et al., 2005; Henjes et al., 2007).

Concluding, the tag pyrosequencing approach in this study has provided an overview of the protistan assemblages present in the naturally fertilized blooms and the HNLC waters in the Southern Ocean. Despite the under-representation of Bacillariophyceae diversity and the over-representation of Dinophyceae in the sequences, the community similarity analysis showed clear differences between the iron-fertilized and the HNLC waters, and among the blooms, in regard to their location and the fertilization mechanisms. The molecular approach has also highlighted a rich assemblage of potential phytoplankton parasites and organic matter decomposers mostly present in the iron-fertilized blooms.

The Supplement related to this article is available online at doi:10.5194/bg-11-5847-2014-supplement.

Acknowledgements. KEOPS was financed by INSU-CNRS, IPEV and ANR and the French Ministry of Higher Education through a PhD grant to C. Georges. We thank our many colleagues who participated in the collection of various data sets, the KEOPS co-ordinator S. Blain, the chief scientist on board B. Quéguiner and the crew aboard the R/V *Marion Dufresne* for their help in the successful completion of the cruise. We also thank www.englisheditor.webs.com for the paper’s English proofing.

Edited by: G. Herndl

References

- Altschul, S. F., Gish, W., Miller, W., Myers, E. W., and Lipman D. J.: Basic local alignment search tool, *J. Mol. Biol.*, 215, 403–410, 1990.
- Amann, R. I., Binder, B. J., Olson, R. J., Chisholm, S. W., Devereux, R., and Stahl, D. A.: Combination of 16S rRNA-targeted oligonucleotide probes with flow cytometry for analyzing mixed microbial populations, *Appl. Environ. Microbiol.*, 56, 1919–192, 1990.
- Armand, L. K., Crosta, X., Quéguiner, B., Mosseri, J., and Garcia, N.: Diatoms preserved in surface sediments of the northeastern Kerguelen Plateau, *Deep Sea Res. II*, 55, 677–692, 2008.
- Arrigo, K. R., Robinson, D. H., Worthen, D. L., Dunbar, R. B., DiTullio, G. R., VanWoert, M., and Lizotte, M. P.: Phytoplankton community structure and the drawdown of nutrients and CO₂ in the Southern Ocean, *Science*, 283, 365–367, 1999.
- Behnke, A., Engel, M., Christen, R., Nebel, M., Klein, R. R., and Stoeck, T.: Depicting more accurate pictures of protistan community complexity using pyrosequencing of hypervariable SSU rRNA gene regions, *Environ. Microbiol.*, 13, 340–349, 2010.
- Bik, H. M., Porazinska, D. L., Creer, S., Caporaso, J. G., Knight, R., and Thomas, K. W.: Sequencing our ways towards understanding global eukaryotic biodiversity, *Trends Ecol. Evol.*, 27, 233–243, 2012.
- Blain, S., Quéguiner, B., Armand, L., Belviso, S., Bombled, B., Bopp, L., Bowie, A., Brunet, C., Brussaard, C., Carlotti, F., Christaki, U., Corbiere, A., Durand, I., Ebersbach, F., Fuda, J. L., Garcia, N., Gerringa, L., Griffiths, B., Guigue, C., Guillermin, C., Jacquet, S., Jeandel, C., Laan, P., Lefevre, D., Lo Monaco, C., Malits, A., Mosseri, J., Obernosterer, I., Park, Y. H., Picheral, M., Pondaven, P., Remenyi, T., Sandroni, V., Sarthou, G., Savoye, N., Scouarnec, L., Souhaut, M., Thuiller, D., Timmermans, K., Trull, T., Uitz, J., van Beek, P., Veldhuis, M., Vincent, D., Viollier, E., Vong, L., and Wagener, T.: Effect of natural iron fertilization on carbon sequestration in the southern ocean, *Nature*, 446, 1070–1074, 2007.
- Blain, S., Quéguiner, B., and Trull, T.: The natural iron fertilization experiment KEOPS (Kerguelen Ocean and Plateau compared Study): an overview, *Deep-Sea Res. II*, 55, 559–565, 2008.
- Blain, S., Oriol, L., Capparos, J., Guéneuguès, A., and Obernosterer, I.: Distributions and stoichiometry of dissolved nitrogen and phosphorus in the iron fertilized region near Kerguelen (Southern Ocean), this volume.
- Boyd, P. W., Law, C. S., Wong, C. S., Nojiri, Y., Tsuda, A., Levasseur, M., Takeda, S., Rivkin, R., Harrison, P. J., Strzepek, R., Gower, J., McKay, R. M., Abraham, E., Arychuk, M., Barwell-Clarke, J., Crawford, W., Crawford, D., Hale, M., Harada, K.,

- Johnson, K., Klyosawa, H., Kudo, I., Marchetti, A., Miller, W., Needoba, J., Nishioka, J., Ogawa, H., Page, J., Robert, M., Saito, H., Sastri, A., Nelson, S., Soutar, T., Sutherland, N., Taira, Y., Whitney, F., Wong, S.-K. E., and Yoshimura, T.: The decline and fate of an iron-induced subarctic phytoplankton bloom, *Nature*, 428, 549–553, 2004.
- Boyd, P. W., Jickells, T., Law, C. S., Blain, S., Boyle, E. A., Bueseler, K. O., Coale, K. H., Cullen, J. J., de Baar, H. J. W., Follows, M., Harvey, M., Lancelot, C., Levasseur, M., Owens, N. P. J., Pollard, R., Rivkin, R. B., Sarmiento, J., Schoemann, V., Smetacek, V., Takeda, S., Tsuda, A., Turner, S., and Watson, A. J.: Mesoscale iron enrichment experiments 1993–2005: Synthesis and future directions, *Science*, 315, 612–617, 2007.
- Bråte, J., Krabberød, A. K., Dolven, J. K., Ose, R. F., Kristensen, T., Bjørklund, K. R.: Radiolaria associated with large diversity of marine alveolates, *Protist*, 163, 767–777, 2012.
- Brussaard, C. P. D., Timmermans, K. R., Uitz, J., and Veldhuis, M. J. W.: Virioplankton dynamics and virally induced phytoplankton lysis versus microzooplankton grazing southeast of the Kerguelen (Southern Ocean), *Deep-Sea Res. II*, 55, 752–765, 2008.
- Caron, D. A., Countway, P. D., Savai, P., Gast, R. J., Schnetzer, A., Moorthi, S. D., Dennett M. R., Moran, D. M. and Jones, A. C.: Defining DNA-based operational taxonomic units for microbial–eukaryote ecology, *Appl. Environ. Microbiol.*, 75, 5797–5808, 2009.
- Caron, D. A., Countway, P. D., Jones, A. C., Kim, D. Y., and Schnetzer, A.: Marine protistan diversity, *Ann. Rev. Mar. Sci.*, 4, 467–493, 2012.
- Christaki, U., Obernosterer, I., Van Wambeke, F., Veldhuis, M. J. W., Garcia, N., and Catala, P.: Microbial food web structure in a naturally iron fertilized area in the Southern Ocean (Kerguelen Plateau), *Deep-Sea Res. II*, 55, 706–719, 2008.
- Christaki, U., Kormas, K. A., Genitsaris, S., Georges, C., Sime-Ngando, T., Viscogliosi, E., and Monchy, S.: Winter-summer succession of unicellular eukaryotes in a meso-eutrophic coastal system, *Microb. Ecol.*, 67, 13–23, this volume.
- Christaki, U., Lefèvre, D., Georges, C., Colombet, J., Catala, P., Courties, C., Sime-Ngando, T., Blain, S., and Obernosterer I.: Microbial food web dynamics during spring phytoplankton blooms in the naturally iron-fertilized Kerguelen area (Southern Ocean), 2014, this volume.
- Clarke, K. R.: Non-parametric multivariate analyses of changes in community structure, *Austr. J. Ecol.*, 18, 117–143, 1993.
- Closset, I., Lasbleiz, M., Leblanc, K., Quéguiner, B., Cavagna, A.-J., Elskens, M., Navez, J., and Cardinal D.: Seasonal evolution of net and regenerated silica production around a natural Fe-fertilized area in the Southern Ocean estimated from Si isotopic approaches, this volume.
- Collado-Mercado E., Radway, J. C., and Collier, J. L.: Novel uncultivated labyrinthulomycetes revealed by 18S rDNA sequences from seawater and sediment samples, *Aquat. Microb. Ecol.*, 58, 215–228, 2010.
- Countway, P. D., Gast, R. J., Dennett, M. R., Savai, P., Rose J. M., and Caron, D. A.: Distinct protistan assemblages characterize the euphotic zone and deep sea (2500 m) of the western North Atlantic (Sargasso Sea and Gulf Stream), *Environ. Microbiol.*, 9, 1219–1232, 2007.
- Countway, P. D., Vigil, P. D., Schnetzer, A., Moorthi, S. D., and Caron, D. A.: Seasonal analysis of protistan community structure and diversity at the USC Microbial Observatory (San Pedro Channel, North Pacific Ocean), *Limnol. Oceanogr.*, 55, 2381–2396, 2010.
- Cullen, J. J.: Hypotheses to explain high-nutrient conditions in the open sea, *Limnol. Oceanogr.*, 36, 1578–1599, 1991.
- DiTullio, G. R., Grebmeier, J. M., Arrigo, K. R., Lizotte, M. P., Robinson, D. H., Leventer, A., Barry, J. P., VanWoert, M. L., and Dunbar, R. B.: Rapid and early export of *Phaeocystis Antarctica* blooms in the Ross Sea, Antarctica, *Nature*, 404, 595–598, 2000.
- Edgar, R. C.: Search and clustering orders of magnitude faster than BLAST, *Bioinformatics*, 26, 2460–2461, 2010.
- Edgcomb, V., Orsi, W., Bunge, J., Jeon, S., Christen, R., Leslin, C., Holder, M., Taylor, G. T., Suarez, P., Varela, R., and Epstein, S.: Protistan microbial observatory in the Cariago Basin, Caribbean, I. Pyrosequencing vs. Sanger insights into species richness, *ISME J.*, 5, 1344–1356, 2011.
- Gilbert, J. A., Steele, J. A., Caporaso, J. G., Steinbruck, L., Reeder, J., Temperton, B., Huse, S., McHardy, A. C., Knight, R., Joint, I., Somerfield, P., Fuhrman, J. A., and Field, D.: Defining seasonal marine microbial community dynamics, *ISME J.*, 6, 298–308, 2012.
- Guillou, L., Viprey, M., Chambouvet, A., Welsh, R. M., Kirkham, A. R., Massana, R., Scanlan, D. J., and Worden A. Z.: Widespread occurrence and genetic diversity of marine parasitoids belonging to Syndiniales (Alveolata), *Environ. Microbiol.*, 10, 3349–3365, 2008.
- Guillou, L., Bachar, D., Audic, S., Bass, D., Berney, C., Bittner, L., Boutte, C., Burgaud, G., de Vargas, C., Decelle, J., Del Campo, J., Dolan, J. R., Dunthorn, M., Edvardsen, B., Holzmann, M., Kooistra, W. H., Lara, E., Le Bescot, N., Logares, R., Mahé, F., Massana, R., Montresor, M., Morard, R., Not, F., Pawlowski, J., Probert, I., Sauvadet, A. L., Siano, R., Stoeck, T., Vaultot, D., Zimmermann, P., and Christen, R.: The Protist Ribosomal Reference database (PR2): a catalog of unicellular eukaryote small sub-unit rRNA sequences with curated taxonomy, *Nucleic Acid Res.*, 41, 597–604, 2013.
- Hall, J. A., and Safi, K.: The impact of in situ Fe fertilization on the microbial food web in the Southern Ocean, *Deep-Sea Res. II*, 48, 2591–2613, 2001.
- Hammer, Ø, Harper, D. A. T., and Ryan, P. D.: PAST: paleontological statistics software package for education and data analysis, *Palaeontol. Electr.*, 4, 1–9, 2001.
- Henjes, J., Assmy, P., Klaas, C., and Smetacek, V.: Response of the larger protozooplankton to an iron-induced phytoplankton bloom in the Polar Frontal Zone of the Southern Ocean (EisenEx), *Deep Sea Res. I*, 54, 774–791, 2007.
- Jürgens, K. and Massana, R.: Protistan grazing on marine bacterioplankton, in: *Microbial Ecology of the Oceans*, edited by: Kirchman, D. L., 2nd Edn., 383–441, 2008.
- Ki, J.-S. and Han, M.-S.: Efficient 5′ ETS walking from conserved 18S rDNA sequences of the dinoflagellates *Alexandrium* and *Akashiwo sanguinea* (Dinophyceae), *J. Appl. Phycol.*, 17, 475–481, 2005.
- Kimura, H. and Naganuma, T.: Thraustochytrids: a neglected agent of the marine microbial food chain, *Aquat. Ecosyst. Health Manag.*, 4, 13–18, 2001.
- Kunin, V., Engelbrektson, A., Ochman, H., and Hugenholtz, P.: Wrinkles in the rare biosphere: pyrosequencing errors can lead

- to artificial inflation of diversity estimates, *Environ. Microbiol.*, 12, 118–123, 2010.
- Landry, M. R., Ondrusek, M. E., Tanner, S. J., Brown, S. L., Constantinou, J., Bidigare, R. R., Coale, K. H., and Fitzwater, S.: Biological response to iron fertilization in the eastern equatorial Pacific (IronEx II). I. Microplankton community abundances and biomass, *Mar. Ecol. Prog. Ser.*, 201, 27–42, 2000.
- Lasbleiz, M., Lefèvre, D., Leblanc, K., and Quéguiner, B.: Biological productivity regime and in-situ methods comparison around the Kerguelen Island in the Southern Ocean, this volume.
- Lie, A. A. Y., Kim, D. Y., Schnetzer, A., and Caron, D. A.: Small-scale temporal and spatial variations in protistan community composition at the San Pedro Ocean Time-series station off the coast of southern California, *Aquat. Microb. Ecol.*, 2, 93–110, 2013.
- López-García, P., Rodríguez-Valera, F., Pedrós-Alió, C., and Moreira, D.: Unexpected diversity of small eukaryotes in deep-sea Antarctic plankton, *Nature*, 409, 603–607, 2001.
- López-García, P., Philippe, H., Gail, F., and Moreira, D.: Autochthonous eukaryotic diversity in hydrothermal sediment and experimental microcolonizers at the Mid-Atlantic Ridge, *P. Natl. Acad. Sci. USA*, 100, 697–702, 2003.
- Magurran, A. E.: *Measuring biological diversity*. Blackwell, Malden, 2004.
- Mangot, J. F., Domaizon, I., Taib, N., Marouni, N., Duffaud, E., Bronner, G., and Debroas, D.: Short-term dynamics of diversity patterns: evidence of continual reassembly within lacustrine small eukaryotes, *Environ. Microbiol.*, 15, 1745–1758, 2013.
- Martin, J. H. and Fitzwater, S. E.: Iron deficiency limits phytoplankton growth in Antarctic waters, *Global Biogeochem. Cy.*, 4, 5–12, 1990.
- Massana, R. and Pedrós-Alió, C.: Unveiling new microbial eukaryotes in the surface ocean, *Curr. Opin. Microbiol.*, 11, 213–218, 2008.
- Massana, R., Terrado, R., Forn, I., Lovejoy, C., and Pedrós-Alió, C.: Distribution and abundance of uncultured heterotrophic flagellates in the world oceans, *Environ. Microbiol.*, 8, 1515–1522, 2006.
- Medinger, R., Nolte, V., Pandey, R. V., Jost, S., Ottenwalder, B., Schlotterer, C., and Boenigk, J.: Diversity in a hidden world: potential and limitation of next-generation sequencing for surveys of molecular diversity of eukaryotic microorganisms, *Mol. Ecol.*, 19, 32–40, 2010.
- Monchy, S., Grattepanche, J. D., Breton, E., Meloni, D., Sancier, G., Chabe, M., Delhaes, L., Viscogliosi, E., Sime-Ngando, T., and Christaki, U.: Microplanktonic community structure in a coastal system relative to a *Phaeocystis* bloom inferred from morphological and tag pyrosequencing methods, *PLoS ONE* 7, e39924, doi:10.1371/journal.pone.0039924, 2012.
- Myklestad, S. M.: Release of extracellular products by phytoplankton with special emphasis on polysaccharides, *Sci. Total Environ.*, 165, 155–164, 1995.
- Nolte, V., Pandey, R. V., Jost, S., Medinger, R., Ottenwälder, B., Boenigk, J., and Schlotterer, C.: Contrasting seasonal niche separation between rare and abundant taxa conceals the extent of protist diversity, *Mol. Ecol.*, 19, 2908–2915, 2010.
- Not, F., Valentin, K., Romari, K., Lovejoy, C., Massana, R., Tobe, K., Vaulot, D., and Medlin, L. K.: Picobiliphytes: a marine picoplanktonic algal group with unknown affinities to other eukaryotes, *Science*, 315, 253–255, 2007.
- Obernosterer, I., Christaki, U., Lefevre, D., Catala, P., Van Wambeke, F., and LeBaron, P.: Rapid bacterial mineralization of organic carbon produced during a phytoplankton bloom induced by natural iron fertilization in the Southern Ocean, *Deep-Sea Res. II*, 55, 777–789, 2008.
- Oliver, J. L., Barber, R. T., Smith, W. O., and Ducklow, H. W.: The heterotrophic bacterial response during Southern Ocean Iron Experiment (SOFEX), *Limnol. Oceanogr.*, 49, 2129–2140, 2004.
- Park, Y. H., Durand, I., Kestenare, E., Rougier, G., Zhou, M., d’Ovidio, F., Cotté, C., and Lee, J. H.: Polar front around the Kerguelen islands: An up-to-date determination and associated circulation of surface/subsurface water, *J. Geophys. Res. Oceans*, 119, doi:10.1002/2014JC010061, 2014.
- Pollard, R., Salter, I., Sanders, R., Lucas, M., Moore, C., Mills, R., Statham, P., Allen, J., Baker, A., and Fones, G.: Southern Ocean deep-water carbon export enhanced by natural iron fertilization, *Nature*, 457, 577–581, 2009.
- Potvin, M. and Lovejoy, C.: PCR-based diversity estimates of artificial and environmental 18S rRNA gene libraries, *J. Eukaryot. Microbiol.*, 56, 174–181, 2009.
- Poulton, A. J., Moore, M., Seeyave, S., Lucas, M. I., Fielding, S., and Ward, P.: Phytoplankton community composition around the Crozet Plateau, with emphasis on diatoms and *Phaeocystis*, *Deep Sea Res. II*, 54, 2085–2105, 2007.
- Prokopowich, C. D., Gregory, T. R., and Crease, T. J.: The correlation between rDNA copy number and genome size in eukaryotes, *Genome*, 46, 48–50, 2003.
- Quéguiner, B.: Iron fertilization and the structure of planktonic communities in high nutrient regions of the Southern Ocean, *Deep Sea Res. Part II Top. Stud. Oceanogr.*, 90, 43–54, 2013.
- Quéroué, F. and Sarthou, G.: The distribution of dissolved trace elements around the Kerguelen plateau region, unpublished KEOPS2 data.
- Quince, C., Lanzen, A., Curtis, T. P., Davenport, R. J., Hall, N., Head, I. M., Read, L. F., and Sloan, W. T.: Accurate determination of microbial diversity from 454 pyrosequencing data, *Nat. Methods*, 6, 639–641, 2009.
- Raghukumar, S.: The role of fungi in marine detrital processes, in: *Marine microbiology: facets and opportunities*, edited by: Ramaiah, N. E., National Institute of Oceanography, Goa, 91–101, 2004.
- Reeder, J. and Knight, R.: The “rare biosphere”: a reality check, *Nat. Methods*, 6, 636–637, 2009.
- Saito, H., Suzuki, K., Hinuma, A., Takahashi, O., Fukami, K., Kiyosawa, H., Saino, T., Saino, T., and Tsuda, A.: Responses of microzooplankton to in situ iron fertilization in the Western Subarctic Pacific (SEEDS), *Prog. Oceanogr.*, 64, 223–236, 2005.
- Sackett, O., Armand, L., Beardall, J., Hill, R., Doblin, M., Connelly, C., Howes, J., Stuart, B., Ralph, P., and Heraud, P.: Taxon specific responses of Southern Ocean diatoms to Fe enrichment revealed by FTIR microspectroscopy, this volume.
- Schloss, P. D., Westcott, S. L., Ryabin, T., Hall, J. R., Hartmann, M., Hollister, E. B., Lesniewski, R. A., Oakley, B. B., Parks, D. H., Robinson, C. J., Sahl, J. W., Stres, B., Thallinger, G. G., Van Horn, D. J., and Weber, C. F.: Introducing mothur: open-source, platform-independent, community-supported software for de-

- scribing and comparing microbial communities, *Appl. Environ. Microbiol.*, 75, 7537–7541, 2009.
- Schloss, P. D., Gevers, D., and Westcott, S. L.: Reducing the effects of PCR amplification and sequencing artifacts on 16S rRNA-based studies, *PLoS ONE*, 6, e27310, doi:10.1371/journal.pone.0027310, 2011.
- Schnepf, E. and Kühn, S. F.: Food uptake and fine structure of *Cryothecomonas longipes* sp. nov., a marine nanoflagellate incertae sedis feeding phagotrophically on large diatoms, *Helgol. Mar. Res.*, 54, 18–32, 2000.
- Schoemann, V., Becquevort, S., Stefels, J., Rousseau, V., and Lancelot, C.: *Phaeocystis* blooms in the global ocean and their controlling mechanisms: a review, *J. Sea Res.*, 53, 43–66, 2005.
- Skovgaard, A., Massana, R., Balague, V., and Saiz E.: Phylogenetic position of the copepod-infesting parasite *Syndinium turbo* (Dinoflagellata, Syndinea), *Protist*, 156, 413–423, 2005.
- Smetacek, V., Assmy, P., and Henjes, J.: The role of grazing in structuring Southern Ocean pelagic ecosystems and biogeochemical cycles, *Antartct. Sci.*, 16, 541–558, 2004.
- Smetacek, V., Klaas, C., Strass, V.H., Assmy, P., Montresor, M., Cisewski, B., Savoye, N., Webb, A., D' Ovidio, F., Arrieta, J. M., Bathmann, U., Bellerby, R., Berg, G. M., Croot, P., Gonzalez, S., Henjes, J., Herndl, G. J., Hoffmann, L. J., Leach, H., Losch, M., Mills, M. M., Neill, C., Peeken, I., Röttgers, R., Sachs, O., Sauter, E., Schmidt, M. M., Schwarz, J., Terbrüggen, A., and Wolf-Gladrow, D.: Deep carbon export from a Southern Ocean iron-fertilized diatom bloom, *Nature*, 487, 313–319, 2012.
- Tillmann, U., Hesse, K.-J., and Tillmann, A.: Large-scale parasitic infection of diatoms in the North Frisian Wadden Sea, *J. Sea Res.*, 42, 255–261, 1999.
- Wolf, C., Frickenhaus, S., Kiliyas, E. S., Peeken, I., and Metfies, K.: Protist community composition in the Pacific sector of the Southern Ocean during austral summer 2010, *Polar Biol.*, 37, 375–389, 2014.
- Zhou, M., Zhu, Y., d'Ovidio, F., Park, Y.H., Durand, I., Kesternare, E., Sanial, E., Van-Beek, P., Quéguiner, B., Carlotti, F., and Blain, F.: Surface currents and upwelling in Kerguelen Plateau regions, 2014.
- Zhu, F., Massana, R., Not, F., Marie, D., and Vaultot, D.: Mapping of picoeucaryotes in marine ecosystems with quantitative PCR of the 18S rRNA gene, *FEMS Microbiol. Ecol.*, 52, 79–92, 2005.